Tectonophysics, 212 (1992) 213–241
Elsevier Science Publishers B.V., Amsterdam

Geology of the d'Entrecasteaux–New Hebrides Arc collision zone: results from a deep submersible survey

J.-Y. Collot [a], S. Lallemand [b], B. Pelletier [c], J.-P. Eissen [c], G. Glaçon [d], M.A. Fisher [e], H.G. Greene [e], J. Boulin [f], J. Daniel [c] and M. Monzier [c]

[a] *ORSTOM -BP 48, 06230 Villefranche / mer, France*
[b] *Université P. et M. Curie, Laboratoire de Géologie Structurale, 4 Place Jussieu, 75252 Paris, France*
[c] *ORSTOM-BP A5, Nouméa, New Caledonia*
[d] *Université de Provence, Laboratoire de Stratigraphie et Paléoécologie, Place Victor Hugo, 13000 Marseille, France*
[e] *U.S. Geological Survey, 345 Middlefield Road, Menlo Park, CA 94025, USA*
[f] *Université de Marseille III Saint Jérôme, Laboratoire de Géologie Structurale, 13397 Marseille, France*

(Received August 16, 1991; revised version accepted April 27, 1992)

ABSTRACT

Collot, J.-Y., Lallemand, S., Pelletier, B., Eissen, J.-P., Glaçon, G., Fisher, M.A., Greene, H.G., Boulin, J., Daniel, J. and Monzier, M., 1992. Geology of the d'Entrecasteaux–New Hebrides Arc collision zone: results from a deep submersible survey. *Tectonophysics*, 212: 213–241.

During the SUBPSO1 cruise, seven submersible dives were conducted between water depths of 5350 and 900 m over the collision zone between the New Hebrides island arc and the d'Entrecasteaux Zone (DEZ). The DEZ, a topographic high on the Australian plate, encompasses the North d'Entrecasteaux Ridge (NDR) and the Bougainville guyot, both of which collide with the island-arc slope. In this report we use diving observations and samples, as well as dredging results, to analyse the geology of the Bougainville guyot and the outer arc slope in the DEZ–arc collision zone, and to decipher the mechanisms of seamount subduction. These data indicate that the Bougainville guyot is a middle Eocene island arc volcano capped with reef limestones that appear to have been deposited during the Late Oligocene to Early Miocene and in Miocene–Pliocene times. This guyot possibly emerged during the Middle and Late Miocene, and started to sink in the New Hebrides trench after the Pliocene. The rocks of the New Hebrides arc slope, in the collision zone, consist primarily of Pliocene–Recent volcaniclastic rocks derived from the arc, and underlying fractured island-arc volcanic basement, possibly of Late Miocene age. However, highly sheared, Upper Oligocene to Lower Miocene nannofossil ooze and chalk are exposed at the toe of the arc slope against the northern flank of the NDR. Based on a comparison with cores collected at DSDP Site 286, the ooze and chalk can be interpreted as sediments accreted from the downgoing plate. East of the Bougainville guyot an antiform that developed in the arc slope as a consequence of the collision reveals a 500-m-thick wedge of strongly tectonized rocks, possibly accreted from the guyot or an already subducted seamount. The wedge that is overlain by less deformed volcaniclastic island-arc rocks and sediments includes imbricated layers of Late Oligocene to Early Miocene reef and micritic limestones. This wedge, which develops against the leading flank of the guyot, tends to smooth its high-drag shape. A comparison between the 500-m-thick wedge of limestones that outcrops southeast of the guyot and the absence of such a wedge over the flat top of the guyot, although the top is overthrust by island-arc rocks and sediments, can be interpreted to suggest that the wedge moves in the subduction zone with the guyot and facilitates its subduction by streamlining.

Introduction

The lithology and structure of collision zones at plate boundaries where a ridge or a seamount underthrusts an island arc provide important keys to understanding both the tectonic processes that shape island arcs and the mechanical properties of the island arc crust. One such collision zone occurs in the SW Pacific Ocean between the New Hebrides island arc and the d'Entrecasteaux Zone, a major submarine chain carried by the Australian plate. The New Hebrides island arc

Correspondence to: J.-Y. Collot, ORSTOM, BP 48, 06230, Villefranche/mer, France.

marks the boundary along which the Australian plate to the west underthrusts the Pacific plate and the North Fiji basin to the east (Fig. 1). The convergence rate between the Australian and Pacific plates is about 10 cm/yr (Minster and Jordan, 1978; Louat and Pelletier, 1989) in an eastward direction (N76°E ± 11°) and the Wadati–Benioff zone dips uniformly about 70° east beneath the New Hebrides island arc (Isacks et al., 1981). According to Carney and Macfarlane (1982), this subduction initiated in the early Late Miocene. The d'Entrecasteaux Zone (DEZ) extends eastward from the northern New Caledonia ridge to where the DEZ collides with the New Hebrides island arc (Pascal et al., 1978; Daniel and Katz, 1981; Collot et al., 1985). Near the trench the DEZ trends slightly oblique (14°) to the plate-convergence direction, so that DEZ creeps northward along the trench at 2.5 cm/yr (Fig. 1). The complex 3-D structure of the arc

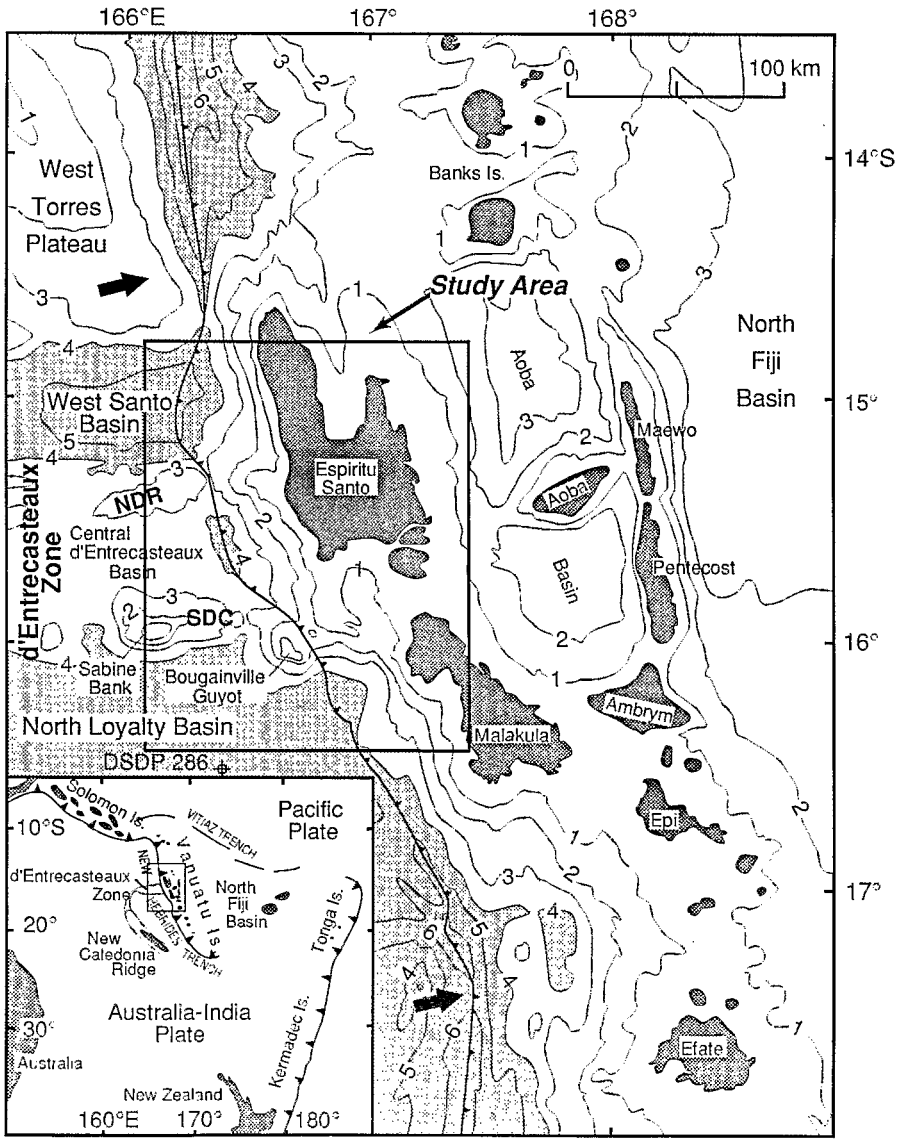

Fig. 1. Location of the study area within the central New Hebrides island arc. *NDR* = North d'Entrecasteaux Ridge; *SDC* = South d'Entrecasteaux Chain. Large arrows show the relative plate motion between the Australian and the North Fiji Basin plates. The bathymetric contour interval is 1 km (after Kroenke et al., 1983).

slope that results from this collision has been described from Seabeam bathymetric data (Daniel et al., 1986; Collot and Fisher, 1989, 1991) and multichannel seismic reflection data (Fisher, 1986; Fisher et al., 1986, 1991a,b). However, little was known about the lithology, age and rocks deformed within this collision zone.

In March 1989, during the SUBPSO1 cruise, the DEZ–New Hebrides island arc collision zone was surveyed using the deep-sea submersible *Nautile* (Collot et al., 1989). This cruise was jointly conducted aboard the *R.V. Nadir* by the Institut Français de Recherche Scientifique pour le Développement en Coopération (ORSTOM) and the Institut Français de Recherche pour l'Exploitation de la Mer (IFREMER). The main objectives of the dives were: (1) to collect rock samples across the arc slope to resolve its lithology and origin; (2) to study the plate contact zone; and (3) to characterize the tectonic style of both the arc slope and the DEZ in the collision zone.

Geologic setting of the DEZ and New Hebrides island arc

West of the New Hebrides island arc, the DEZ strikes east–west and bifurcates into the North d'Entrecasteaux Ridge (NDR) and the South d'Entrecasteaux Chain (SDC) (Fig. 1). The NDR rises 3000 m locally above the abyssal plain and consists of horsts of latest Paleocene to Early Oligocene mid-ocean ridge basalt (MORB) (Maillet et al., 1983), which is overlain by stratified volcaniclastic sediments (Fisher et al., 1991a). The SDC includes two flat-topped seamounts, the Bougainville guyot and the Sabine bank, which are aligned with two smaller conical seamounts. The Sabine bank rises nearly to sea level, whereas the Bougainville guyot lies at a water depth of 1000–1500 m and clogs the trench. This guyot is 3000 m high and is topped by a reefal platform that is tilted 5° arcward (Daniel et al., 1986). Multichannel seismic reflection data have revealed that this platform is approximately 700 m thick and that a 2-km-thick, well stratified debris apron underlies the guyot' s flanks (Fisher et al., 1986, 1991b).

The DEZ separates the West Santo basin to the north from the North Loyalty basin to the south (Fig. 1). The West Santo basin underlies water as deep as 5000 m and contains about 1.5 km of sediments that overlie oceanic crust of unknown age (Pontoise and Tiffin, 1986; Collot and Fisher, 1991).

The North Loyalty basin, under 4500 m of water, formed as a marginal basin during the Late Paleocene to Late Eocene (Andrews et al., 1975; Weissel et al., 1982). Deep Sea Drilling Project (DSDP) Site 286 (Andrews et al., 1975), located 50 km south of the DEZ (Fig. 1), revealed 650 m of sediments overlying basaltic pillow lavas and gabbro. Drilling results show that, during the Middle and Late Eocene, alternating siltstone and sandstone containing pumice and volcanic glass of andesitic affinity was rapidly deposited on the oceanic basement. This volcanic series includes a coarse andesite conglomerate, suggesting that, during the Middle Eocene, the location of Site 286 was proximal to an island arc (Maillet et al., 1983). During the latest Eocene sedimentation changed sharply from the volcanic series to overlying nannofossil ooze and chalk, with minor amounts of ash. The calcareous sedimentation continued during Oligocene times, suggesting a deepening of the sea floor. This deepening may have intensified during the latest Oligocene or Early Miocene, as indicated by the deposition of abyssal red clays. The absence of Miocene sediments points to either non-deposition or erosion before deposition of Pliocene and Pleistocene deep-water sediments.

The central New Hebrides island arc includes three north-trending belts of islands: the western belt exposed along the Espiritu Santo and Malakula Islands, the central belt represented by Aoba and Ambrym islands, and the eastern belt evident on Maewo and Pentecost islands (Fig. 1). All three belts have foundations composed of island-arc volcanic rocks. The western belt is thought to have originated during the Late Oligocene (?)–Early Miocene along a subduction zone that faced east (Mitchell and Warden, 1971; Carney and Macfarlane, 1982; Greene et al., 1988). During the Early to lower Middle Miocene (Fig. 2), this subduction gave rise to volcanos that

were flanked by fringing reefs and surrounded by thick volcaniclastic deposits (Mallick and Greenbaum, 1977). Volcanic intrusions dated from the latest Early to the early Middle Miocene were associated with this phase of volcanism (Carney et al., 1985). During the Middle Miocene, volcaniclastic sediment that was derived from uplifted volcanic basement, as well as reefal limestone, was deposited in subsiding basins along the western belt. From the end of the Middle Miocene to the latest Miocene the western belt was uplifted and eroded. Detrital material derived during this erosion was probably deposited along what is now the trench slope that lies west of Espiritu Santo island. When the North Fiji basin began to form during the Late Miocene (Malahoff et al., 1982; Auzende et al., 1988), the volcanic axis shifted from the western to the eastern belt; this shift may have been caused by a flip of subduction polarity, from east-facing to west-facing (Chase, 1971; Falvey, 1975). The present accretionary complex could have begun to form following this polarity flip. By the end of the Miocene, a marine transgression had deposited hemipelagic and pelagic calcareous sediments unconformably on top of the older rocks of the western belt (Macfarlane et al., 1988). During the Pliocene, when the volcanism shifted westward from the eastern belt to the central belt, the western belt again started to rise and became covered by successive reef terraces (Mallick and Greenbaum, 1977; Carney and Macfarlane, 1980). This uplift, which may have resulted from collision with the DEZ, reached a maximum rate of 5–6 mm/yr during the Holocene (Taylor et al., 1980, 1985, 1987; Jouannic et al., 1980) and formed high (1800 m) mountains on Espiritu Santo island. Consequently, sediment eroded from Espiritu Santo island since the Pliocene could have contributed significantly to deposits of the eastern trench slope.

West of Espiritu Santo island, the trench slope has been severely deformed by the collisions of the NDR and the Bougainville guyot (Fig. 2). The oblique collision of the NDR against the arc has produced an asymmetric tectonic pattern in arc slope rocks (Collot and Fisher, 1991). This pattern is characterized by three features: (1) N120°-trending strike-slip lineaments north of the NDR; (2) the highly uplifted Wousi bank east of the NDR; and (3) E–W-trending normal faults south of the ridge. South of the NDR, the ongoing collision with the Bougainville guyot has produced a 10-km indentation in the arc slope (Daniel et al., 1986). Uplift and thrust faulting concomitant with this indentation have produced an antiform in the arc slope that towers 800 m over the guyot (Fisher et al., 1986, 1991b).

Lithology, age and structure of rocks in the collision zone

Geologic data collected during the dives across major seafloor scarps of the DEZ–New Hebrides island arc collision zone were augmented by samples that were dredged from along the NDR during the GEORSTOM III cruise (1975) and along the Bougainville guyot during the SEAPSO 1 cruise (1985). In the next four sections, the NDR and Bougainville guyot collision zones are described. For each collision zone, we first present and interpret the geologic data from the downgoing plate, and then from the adjacent arc slope. In this report we use the sediment and sedimentary rock classification employed by the Ocean Drilling Program (Mazzullo et al., 1987). Lithologic, age and geochemistry data are presented in Tables 1, 2 and 3.

The North d'Entrecasteaux Ridge (NDR)

The summit of the North d'Entrecasteaux Ridge was explored during dive 2 (Fig. 2). The ridge has a smooth morphology and is blanketed with a silty clay of Late Pleistocene to Recent age (Table 1); however, Oligocene and Miocene pelagic microfossils are common in this clay. Several rock samples dredged from the flanks of the NDR about 120 km west of the collision zone (Maillet et al., 1983) revealed Late Pliocene and Late Pleistocene clay (Go314–315 in Table 2).

The arc slope in front of the North d'Entrecasteaux Ridge

During dive 1 of the *Nautile*, the upper arc slope adjacent to the NDR was surveyed along

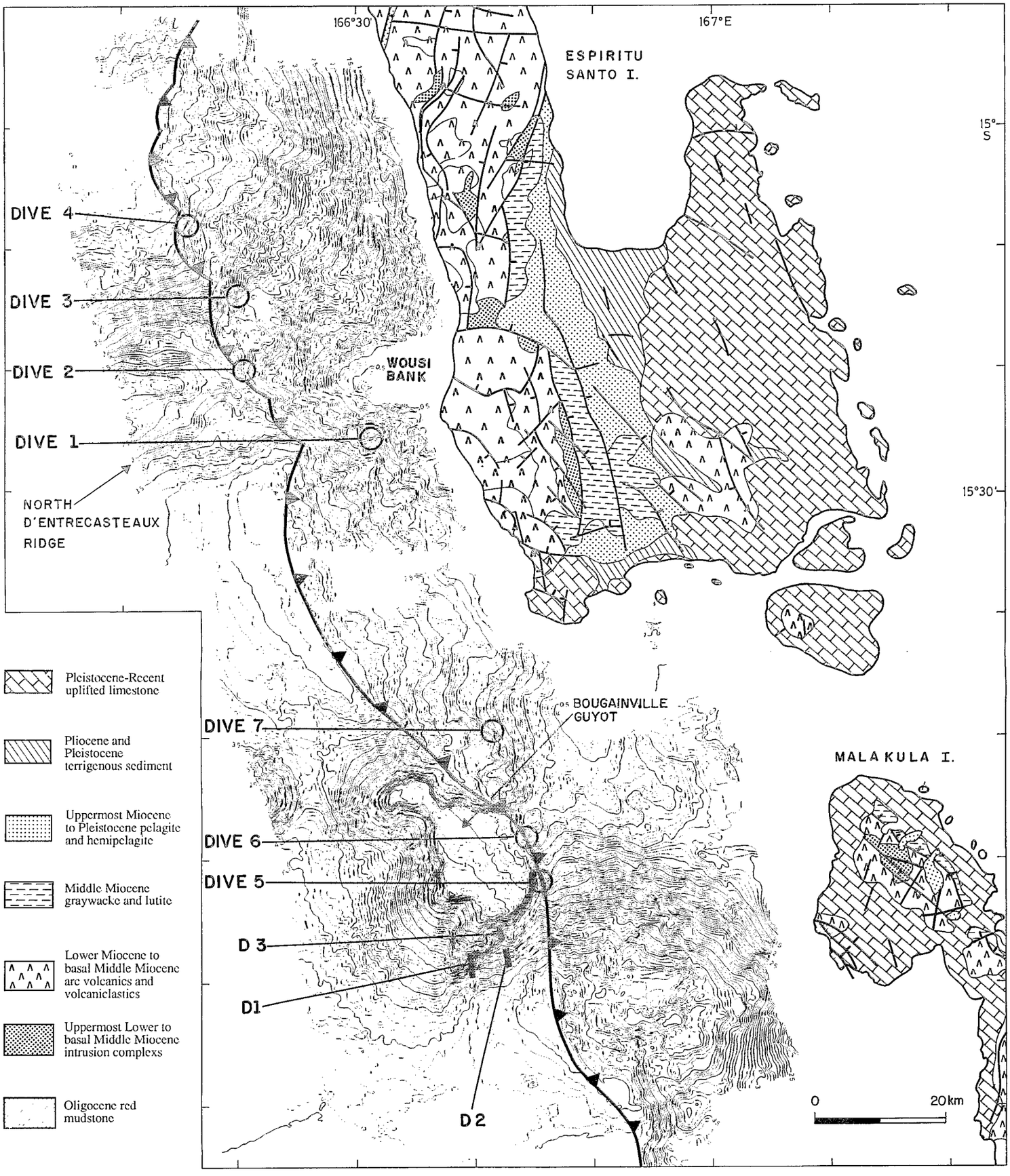

Fig. 2. Simplified geologic map of Espiritu Santo and Malakula islands (after Carney and Macfarlane, 1982) and Seabeam bathymetric map of the collision zone between the d'Entrecasteaux Zone and the New Hebrides island arc (after Daniel et al., 1986). The location of this area is shown in Fig. 1. Dive 1 indicates the location of a dive conducted during the SUBPSO1 cruise; D1 indicates a dredging site from the SEAPSO1 cruise.

TABLE 1

Description and biostratigraphy of samples collected in the d'Entrecasteaux Zone—New Hebrides island arc collision zone during the SUBPSO1 cruise (1989). Pliocene (Miocene) = Pliocene sediment including reworked Miocene; biostratigraphy is based on Berggren et al. (1985); lithology is based on Mazzullo et al., (1987); carbonate facies are from L. Montaggioni; scleractinian determination from G. Faure; MSR = mixed sedimentary rock

Sample no.	Depth (m)	Description	Age [a]
North d'Entrecasteaux Ridge Zone			
Dive 1			
101	2084	Gray polygenetic volcanic breccia	?
102	2086	Reefal limestone	?
103	2087	Weathered reddish andesite	?
104	2090	Coral	?
105	2074	Weathered reddish andesite	?
106	2042	Gray coarse polygenetic volcanic breccia	?
107	1956	Gray polygenetic volcanic breccia	?
108	1954	Reddish gray andesitic basalt	?
109	1903	Gray volcanic sandstone	?
110	1880	Greenish gray volcanic sandstone	?
111	1835	Gray highly phyric andesitic basalt	7.3 ± 0.36 Ma (K/Ar)
112	1742	Greenish gray volcanic sandstone	?
Dive 2			
201	3060	Greenish brown calcareous silty clay	Late Pleistocene–Holocene NN21(early Middle Miocene NN4–NN5) (N, P)
202	2870	Greenish brown calcareous silty clay	Late Pleistocene–Holocene NN 20–21(early Middle Miocene NN4–NN5, Pliocene) (N, P)
203	2870	Greenish brown calcareous silty clay	Pleistocene NN20–21 (Latest Miocene NN11, early Middle Miocene NN5) (N, P)
204	?	Greenish brown calcareous silty clay	Late Pleistocene NN20–21 (Oligocene, early Middle Miocene NN4-NN5, Pliocene) (N, P)
Dive 3			
301	3426	Dark gray volcanic sandstone	?
302	3372	Pale brownish silty clay foram MSR with nannofossils	Late Pliocene NN18 (N, P)
303	3364	Dark grayish brown poorly consolidated volcanic breccia	?
304A	3365	Light brown calcareous volcanic clayey siltstone	Latest Miocene NN11b (early Middle Miocene NN4–NN5) (N), Early Pliocene (P)
304B	3365	Light brown calcareous volcanic clayey siltstone	Late Miocene NN11a (N, P)
305	3262	Dark gray unconsolidated volcanic breccia	?
306	3267	Brown calcareous volcanic silty clay with volcanic and chalk clasts	Late Pliocene–Quaternary (P), Latest Miocene NN11b (N)
307	3260	Light gray silty clay nannofossil foram MSR	Early Pleistocene NN19 (Pliocene, Middle Miocene) (N, P)
308	3211	Light brown silty clay nannofossil foram MSR	Late Pliocene NN16 (N), Late Quaternary (P)
309	3191	Grayish calcareous volcanic clayey siltstone	Late Pleistocene NN20 (Pliocene) (N, P)
310	3194	Light gray sandy biograinstone	Pliocene–Quaternary (P)
311	3134	Light brown calcareous volcanic clayey siltstone	Latest Miocene NN11 (early Middle Miocene NN4–NN5) (N), Late Quaternary (P)
312	3022	Brownish silty clay foram MSR with nannofossils	Early Pleistocene NN19 (N, P)
313A	3023	Light grayish brown foram clayey silt MSR	Early Pleistocene NN19 (N, P)

TABLE 1 (continued)

Sample no.	Depth (m)	Description	Age [a]
313B	3023	Light brown gray foram clayey silt MSR	Late Pleistocene NN21 (Late Miocene, Pliocene) (N, P)
314	2826	Brownish gray foram silty clay MSR	Late Pleistocene NN20–21 (Pliocene) (N)
318	2836	Brownish volcanic breccia with basaltic clasts	clast: 16.04 ± 0.8 Ma (K/Ar)
Dive 4			
401	5349	Light gray silty clay foram MSR	Early Pleistocene NN19 (Pliocene) (N, P)
402	5159	Very pale brown clayey nannofossil ooze	Middle Oligocene NP 23 (Eocene) (N) Late Pliocene–Quaternary (P)
403	5108	Very pale brown clayey nannofossil ooze	Early Miocene NN2 (Oligocene) (N), Late Pliocene-Quaternary (P)
404	5071	Pale brown clayey nannochalk with silt spicule	Early Miocene NN1–2 (N), Late Miocene–Recent (P)
405	5068	Light olive gray silty clay foram MSR	Late Pliocene NN18 (N), Early Pliocene (P)
406	5065	Very pale brown clayey nannofossil chalk with spicule	Uppermost Oligocene, Early Miocene NN2 (N), Late Pliocene–Quaternary (P)
407	5003	Pale brown silty clayey nannofossil ooze	Middle Oligocene NP23 (N), Pliocene (P)
408A	4882	Pale brown nannofossil foram clayey silt MSR	Pleistocene (P), Oligocene, Early Miocene (N)
408B	4882	Light gray nannofossil foram clayey silt MSR	Late Pliocene NN16 (N, P)
409	4810	Grey calcareous silty clay with clasts of very pale brown chalk	Late Pliocene NN16 (Oligocene–Miocene) (N, P)
410A	4705	Light gray clayey silt nannofossil foram MSR	Late Pliocene NN17 (N, P)
410B	4705	Light gray silty clay nannofossil foram MSR	Early Pliocene NN15 (N), Late Pliocene–Quaternary (P)
410C	4705	Light olive gray calcareous volcanic sandy clayey siltstone	Late Pleistocene NN20–21 (Middle–Late Miocene, Pliocene) (N, P)
411	4523	Pale brown clayey nannochalk with silt spicule	Early Miocene NN1 (N), Late Miocene–Recent (P)
Bougainville Zone			
Dive 5			
501	2082	Encrusted reef grainstone to wackstone	Middle Eocene to Present (B)
502	2087	Coral colony fragment	?
503	2295	Coral colony fragment	?
504	2329	White fine limestone with foram	?
505	2327	Reddish yellow foram volcanic coarse semi-consolidated sandstone	Late Eocene to Early Oligocene (Ca)
506	2214	White fine limestone with foram	?
507	2095	Brownish white foram packstone with plagioclases	Early Oligocene NP 21 (N), late Oligocene–early Miocene (Late Eocene) (B)
508	2059	Grayish white biopackstone with large foram and ooze filling	?, filling: Late Pliocene–Quaternary (P)
509	1905	Olive gray calcareous volcanic sandstone with foram	Early Pliocene NN15 (N, P)
510	1706	Olive gray calcareous volcanic clayey siltstone with foram and spicule	Late Pleistocene NN21- Holocene (N, P)
Dive 6			
601	1676	White reef wackstone with ooze filling	Miocene–Pliocene (B), filling: Pliocene (P)
602A	1620	Pale brown clayey limestone with foram and spicule	Miocene–Pliocene (N, P)
602B	1620	Light olive gray calcareous volcanic clayey siltstone	Latest Miocene NN11 (early Middle Miocene NN5) (N), Pliocene–Pleistocene (P)
603A	1623	microlitic basalt	9.42 ± 0.47 Ma (K/Ar)
603B	1623	Pale brown clayey nannofossil limestone with foram and spicule	Late Oligocene NP25 (N, P)
603C	1623	White foram packstone	Late Oligocene NP25 (N, P) (Middle Eocene) (P)

TABLE 1 (continued)

Sample no.	Depth (m)	Description	Age [a]
604A	1602?	Olive gray calcareous volcanic sandy siltstone	Late Pliocene NN16 (N, P) (Miocene–Pliocene) (P)
604B	1602?	Very pale brown clayey nannofossil chalk with foram and spicule	Early Miocene NN3 (N), Late Miocene–Recent (Middle Oligocene) (P), Late Miocene–Pliocene (O)
604C	1602?	Pumice boulder	?
605	1590?	Olive gray calcareous volcanic sandy siltstone	Quaternary (Latest Miocene NN11) (N), Late Pliocene to Recent (Late Miocene) (P)
606	1590?	Serpentinized lherzolite	?
607	1240?	Gray sandy biograinstone (rhodolithe)	Early Miocene (B)
Dive 7			
701	2258	Dark olive gray calcareous silty clay	Late Pleistocene NN21 (Mio-Pliocene) (N, P)
702	2213	Dark olive gray volcanic sandstone	?
703	2000	Gray volcanic sandstone	?
704	1974	Grayish brown calcareous volcanic siltstone	Late Pleistocene–Holocene NN20–21 (Mio-Pliocene) (N)
705	1974	Phyric andesite from a conglomerate	16.6–17 ± 0.8 Ma (K/Ar)
706	2000	Olive gray calcareous silty clay with chalk and volcanic clasts	Late Pleistocene–Holocene NN21 (N, P) (Oligocene, Pliocene) (N)
707	2000	Dark gray volcanic sandstone	?

[a] K/Ar ages (fide H. Bellon); N: planktonic nannofossils (fide C. Muller); P: planktonic foramminifers (fide G. Glaçon); B: large benthic foraminifers (fide J. Butterlin); Ca: Camerinidae (fide A. Blondeau), O: Ostracods (fide J. F. Babinot).

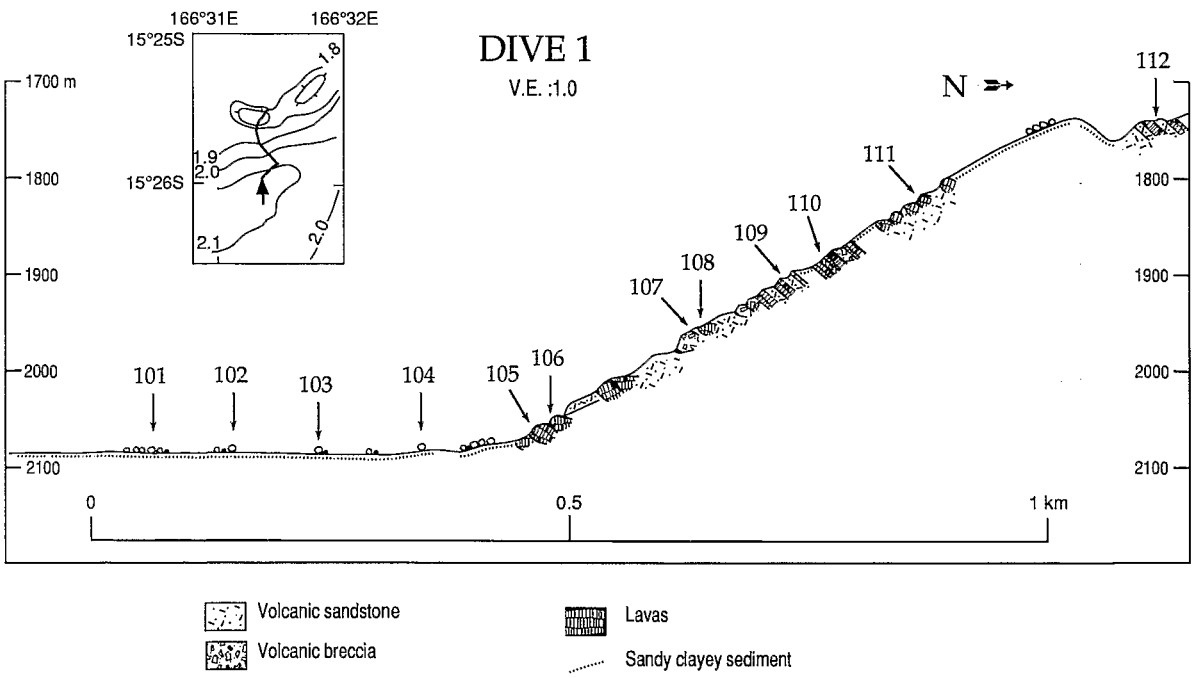

Fig. 3. Interpreted geologic cross-section of a scarp of the New Hebrides arc slope along the south flank of the Wousi bank (dive 1); location in Fig. 2; inset is *Nautile* traverse; arrows with numbers indicate location of samples described in Table 1.

the south flank of the Wousi bank. During dives 2, 3 and 4 the toe of the arc slope was explored east and north of the NDR (Fig. 2).

The upper arc slope east of the NDR

Dive 1 began on a subhorizontal platform and rose along a steep (30°), south-facing slope (Fig.

TABLE 2

Description and biostratigraphy of samples dredged along the d'Entrecasteaux Zone. Go 314–315 are from the GEORSTOM III Nord (1975) cruise; D1, D2, D3 are from the SEAPSO1 (1985) cruise; for legend see Table 1

Dredge no.	Sample no.	Depth (m)	Description	Age [a]
North d'Entrecasteaux Ridge				
Go314	D16	3120–2800	Light brown calcareous clay	Late Pleistocene NN21 (N, P)
Go315	D15	2160–1800	Light brown foraminiferal clay	Late Pliocene NN16 (N, P)
Bougainville guyot				
D1	A	2800–2300	Volcanic breccia	?
	B	2800–2300	Olivine porphyritic basalt	?
	C	2800–2300	Olivine porphyritic basalt	?
	D	2800–2300	Gray volcanic microconglomerate	?
	E	2800–2300	Porphyritic basaltic andesite	?
	F	2800–2300	Olivine porphyritic basalt	?
	G	2800–2300	Microcrystalline basalt	?
	H	2800–2300	Porphyritic basaltic andesite	15.0? ± 0.8 (K/Ar) (altered sample)
	I	2800–2300	Volcanic breccia, chalky matrix	Uppermost Middle Eocene NP17 (N)
	J	2800–2300	Volcanic, carbonate conglomerate	Middle Oligocene (N), Late Oligocene–Early Miocene (B)
	K	2800–2300	Volcanic breccia, carbonate matrix	?
	L	2800–2300	Carbonate breccia	Uppermost Miocene–Early Pliocene (B), Late Middle Oligocene (N), Late Oligocene–Early Pliocene (P)
	M	2800–2300	Scleractinian (Leptastrea)	Oligocene to Recent
D2	A	3650–3320	Gray white nannofossil foram chalk and clay	Late Pleistocene NN20 (N, P)
	B1	3650–3320	Gray white nannofossil foram chalk and clay	Late Pleistocene NN20 (N, P), (Late Eocene–Early Miocene) (P)
	B2	3650–3320	Gray white nannofossil foram chalk and clay	Late Pleistocene NN20 (N, P)
	C	3650–3320	Gray bedded chert	?
	D	3650–3320	Greenish brown silty clay	Late Pleistocene NN21 (N, P)
	E	3650–3320	Coral fragment	?
	F	3650–3320	Coral fragment (Platygyra)	Eocene to Recent
	G	3650–3320	Reef packstone	Late Oligocene–Early Miocene (B)
	H	3650–3320	Coral fragment	?
	I	3650–3320	Reef packstone	Late Eocene to Recent (B)
	J	3650–3320	Fresh coral fragments	Eocene to Recent
D3	A	2100–1800	Brown silty clay and neretic foram	Late Pleistocene NN21 (N) Holocene (P)
	B	2100–1800	Reef packstone with halimeda	?
	C	2100–1800	Reef grainstone/packstone	?
	D	2100–1800	Reef packstone	?
	E	2100–1800	Reef grainstone/packstone	?

[a] K/Ar ages (fide H. Bellon); N: planktonic nannofossils (fide C. Muller); P: planktonic foramminifers (fide G. Glaçon); B: large benthic foraminifers (fide J. Butterlin)

3). The platform is covered with mud, sand and transported boulders of andesite, coral, reefal limestone and volcanic breccia, together with wood and land-born vegetation debris. These observations suggest debris flow deposition. The south-facing slope shows a series of flats interspersed with southward-dipping sedimented slopes, and 40–70° steep scarps that trend N20–90°. Rock outcrops along the scarps reveal fractured volcanic breccia, volcanic sandstone and lava. Several outcrops show large blocks (1–2 m) of lavas in a chaotic volcaniclastic mass that suggests olistostrome deposits; however, some massive outcrops of lava (Plate I-1) could represent coherent lava flows that are interbedded with volcaniclastic layers. Most these lavas are dominantly plagioclase-rich, one or two pyroxene, phyric andesites; island-arc basalt tholeiite and dacite fragments were also recovered from the breccias (Table 3). One andesite (111, Table 1) was radiometrically dated and yielded a Late Miocene age. Massive lava and volcaniclastic beds locally dip 30–40°NE and strike N120°, and are affected by N30–50°-trending fractures that dip 20°N to subvertical.

The contact zone and the toe of the arc slope above the NDR

The contact zone between the arc slope and the summit of the NDR is marked by a west-facing, 1–2-m-high scarp that trends N155° and exposes slightly indurated clay (dive 2, Fig. 2). At this location, the sea floor over the toe of the arc slope dips 25–45° W and is blanketed by a fractured, silty clay of Pleistocene to Holocene age (Table 1).

About 4 km east of the contact zone, a major 250-m high, north-facing scarp reveals the internal structures of the arc slope above the subducted part of the NDR (Dive 3, Fig. 4). Observations made during dive 3 indicate that the scarp towers above a gently north-dipping seafloor that is incised by N20–40°-trending channels. This sea floor consists of stratified clayey siltstone that is overlain by a debris cone. The major scarp slopes 25° north and has walls as steep as 70–80°.

Exposed at the scarp are Late Pliocene to Quaternary, calcareous, deep-water rocks that have a volcaniclastic component; these rocks are interbedded with volcanic breccias (dive 3, Table 1). A clast of island-arc tholeiite (sample 318 in

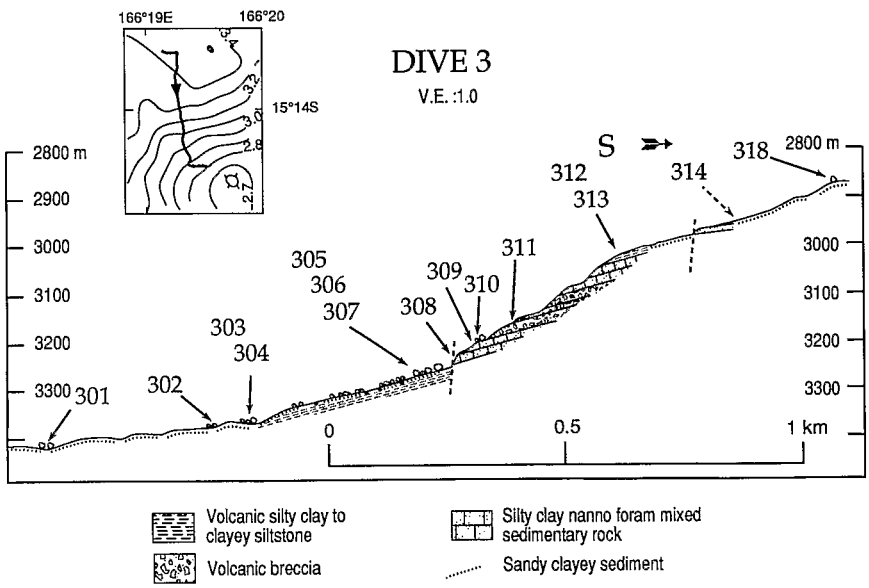

Fig. 4. Interpreted geologic cross-section of a scarp of the New Hebrides arc slope above the North d'Entrecasteaux Ridge (dive 3); location in Fig. 2; inset is *Nautile* traverse; arrows with numbers indicate location of samples described in Table 1.


1

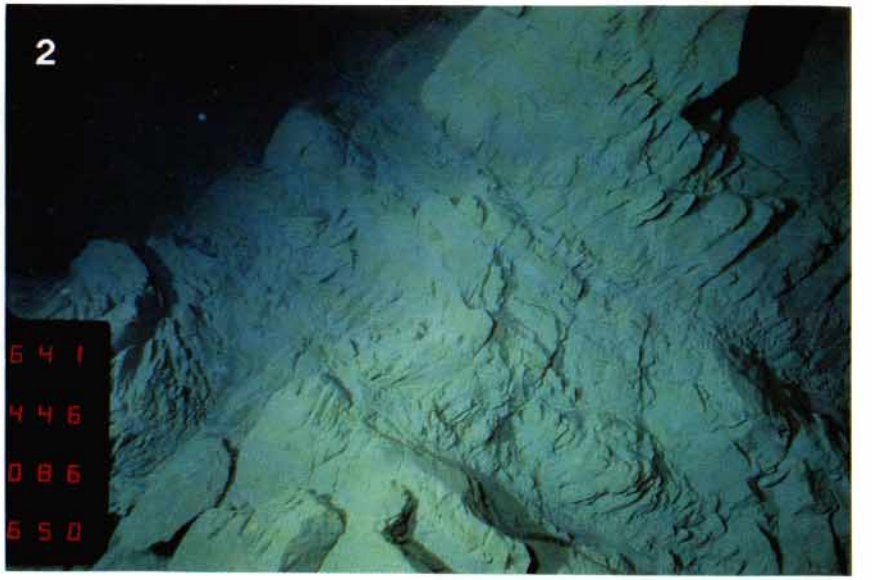
2


3


4

Table 3) obtained from a volcanic breccia, yielded an early Middle Miocene K/Ar age (Table 1) that is coeval with the volcanism of the western belt of the New Hebrides island arc (Fig. 2).

Structural data show that, along the scarp, rocks are fractured and locally folded on a small scale; these rocks strike N120° and dip 20–40°N. This northward dip could have been caused as rocks that dipped trenchward were progressively uplifted as the NDR crept north during the collision. Subvertical fractures trending N120–140° were observed in rock outcrops and appear to parallel the N120° trending strike-slip faults that have been interpreted from Seabeam bathymetric data (Collot and Fisher, 1991).

The toe of the arc slope north of the NDR

The arc slope adjacent to the lower northern flank of the NDR has a lobate morphology (Fig. 2) and appears to be offset left-laterally along a N120° trending strike-slip fault (Collot and Fisher, 1991). The lower northern flank of the NDR rises gently (8°) southward, is overlain by sand, and scattered boulders and gravels (dive 4, Fig. 5). The toe of the arc slope rises 650 m southeastward at an angle of 18° and shows an uneven morphology with steep (50–70°) scarps. The morphology suggests that outcrops were sculpted by down slope transport of sediment (Greene et al., 1992).

Rock outcrops at the toe of the arc slope consist of deformed, layered Pliocene to Quaternary calcareous volcanic siltstone and mixed sedimentary rocks, and Oligocene–Miocene clayey nannofossil ooze and chalk (dive 4, Table 1). This last age is questionable because planktonic foraminifers recovered from the ooze and chalk provide Pliocene–Quaternary ages, whereas nannofossils from the same samples indicate ages older than Early Miocene. Because of the considerable amount of nannofossils in the samples, we infer that Oligocene–Miocene clayey nannofossil ooze and chalk outcrop at the sea floor (Fig. 5). Nevertheless, a Late Pliocene sedimentary melange including clasts of Oligocene–Miocene chalk is evident near the depth of 4800 m (409, Table 1).

Where the lower northern flank of the NDR enters the subduction zone, arc slope rocks dip arcward 45–70° and are strongly tectonized. Rocks are sheared and fractured (Plate I-2); shear zones that dip east (Fig. 5) often parallel the bedding plane and are interpreted as thrusts. Near 5050 m, a subvertical fault trending N110° is subparallel to both the N120–140° directions of subvertical fractures measured upslope (dive 3) and the strike-slip faults interpreted from Seabeam morphologic data. Structural observations such as fresh fractures and slump scars are indicative of present-day tectonic activity (Greene et al., 1992). Age and lithologic data, together with structural observations, suggest that a sequence of both Late Pleistocene siltstone and Early Pliocene to Quaternary mixed sedimentary rocks is sandwiched between the Oligocene–Miocene nannofossil ooze and chalk (Fig. 5).

Rock outcrops frequently exhibit white mineralized patches and veins. These mineralizations may relate to dewatering process of the accretionary complex (Plate I-3).

The Bougainville guyot

The platform and the shallow part of the SE flank of the Bougainville guyot were explored during dives 6 and 5; furthermore, three dredging hauls were obtained along the south flank of the guyot (Fig. 2).

Plate I

1 Fractured, massive andesite exposed along the south flank of the Wousi bank (dive 1, 1954 m).

2 Fractured and sheared calcareous volcanic siltstone at the lower arc slope against the northern flank of the North d'Entrecasteaux Ridge (dive 4, 4650 m).

3 Sheared and veined brown ooze and chalk at the toe of the arc slope against the northern flank of the North d'Entrecasteaux Ridge (dive 4, 5103 m). The white patch may indicate mineral deposits that result from compressional dewatering.

4 Miocene–Pliocene reef limestone on the summit platform of the Bougainville guyot; note the dissolution features (dive 6, 1480 m).

TABLE 3

Bulk rock analysis of lavas from the collision zone between the New Hebrides island arc and the d'Entrecasteaux Zone. SBS 1 = SUBPSO1 cruise; SPS 1 = SEAPSO1 cruise; IAT = island-arc tholeiite; BA = basic andesite; A = andesite; MORB = mid-ocean ridge basalt; PER = peridotite; VS = volcanic sandstone; FeO* = FeO total; Mg# = 100 × Mg/(Mg+Fe); major and trace elements were analysed by Atomic Absorption, except Sc, Y, Zr, and Nb analyzed by inductively coupled plasma emission spectrometry.

Cruise	SBS 1	SBS 1	SBS 1	SBS 1	SBS 1	SBS 1	SBS 1	SBS 1	SPS 1	SPS 1	SPS 1	SPS 1	SPS 1	SPS 1	SPS 1
Sample no.	106	111	318	705	603A	606	301	703	D1H	D1K	D1E	D1G	D1B	D1C	D1F
Rock type	IAT	BA	IAT	A	MORB	PER	VS	VS	BA	A	BA	IAT	IAT	IAT	IAT
SiO_2	47.85	52.30	48.00	55.70	48.50	39.70	56.65	51.60	53.00	54.20	54.40	48.65	46.60	42.05	46.80
TiO_2	0.98	1.07	0.75	0.86	1.60	0.01	0.95	0.95	0.96	0.87	0.91	1.15	0.75	0.68	0.36
Al_2O_3	18.13	16.82	20.60	17.21	14.79	1.11	17.40	17.75	19.42	16.82	17.35	16.55	16.68	15.78	11.47
Fe_2O_3	10.17	9.38	8.78	7.77	10.68	8.24	5.14	8.80	7.77	7.47	7.58	9.49	10.20	8.29	7.77
MnO	0.18	0.18	0.15	0.12	0.15	0.09	0.09	0.13	0.12	0.11	0.07	0.11	0.09	0.14	0.11
MgO	5.97	4.29	4.86	2.61	6.75	35.10	2.07	3.64	3.54	3.77	3.95	2.78	4.54	3.46	14.00
CaO	10.63	7.86	8.53	7.47	9.97	0.57	5.89	7.46	9.12	6.85	7.20	9.96	11.86	16.09	9.70
Na_2O	2.59	3.60	3.96	3.74	2.81	0.07	4.09	3.70	3.78	3.61	4.68	4.29	3.01	2.79	1.71
K_2O	0.39	0.89	0.36	1.27	0.71	0.04	1.38	0.61	0.34	0.62	0.45	0.50	0.44	0.63	0.26
P_2O_5	0.10	0.12	0.05	0.15	0.10	0.00	0.05	0.10	0.15	0.15	0.15	1.70	1.00	0.40	0.10
H_2O^+	2.32	2.74	2.70	1.30	2.27	12.65	4.27	3.87	1.08	3.40	1.04	1.97	2.73	7.55	3.58
H_2O^-	0.15	0.30	0.72	0.96	1.25	1.19	1.76	1.37	1.07	1.61	1.31	2.10	1.90	1.28	3.47
Total	99.46	99.55	99.46	99.16	99.58	98.77	99.74	99.98	100.35	99.48	99.09	99.25	99.80	99.14	99.33
FeO*/MgO	1.32	1.69	1.40	2.31	1.23	0.18	1.92	1.87	1.70	1.53	1.49	2.64	1.74	1.86	0.43
Mg#	54.3	48.1	52.9	40.5	56.1	89.6	44.9	45.6	48.0	50.6	51.4	37.2	47.4	45.8	78.5
Li	11	7	10	12	44	10	12	37	16	15	27	19	18	13	51
Rb	6	8	7	23	12	2	11	7	4	7	6	8	6	8	4
Sr	471	530	486	365	144	9	554	433	400	324	365	448	715	316	222
Ba	76	138	35	227	15	10	105	116	25	40	30	45	40	50	25
V	287	237	207	190	279	21	204	210	208	168	210	225	246	212	140
Cr	45	20	15	2	198	2250	9	10	21	48	50	10	325	272	571
Co	30	21	27	24	39	86	14	25	41	36	32	30	36	48	53
Ni	31	21	28	23	99	2050	23	21	20	41	14	20	80	162	163
Cu	71	138	69	53	47	10	41	53	64	78	76	89	75	84	72
Zn	72	85	57	82	82	35	63	85	68	66	70	107	111	81	95
Sc	39.4	28.5	22.8	17.5	36.6	9.4	24.8	25.6	24.9	24.3	23.2	29.4	29.5	28.3	37.9
Y	19.0	29.4	16.8	26.3	34.4	0.1	18.3	24.9	20.0	17.6	19.8	27.3	15.9	17.1	8.5
Zr	41	104	41	99	84	4	44	71	75	95	97	105	83	50	31
Nb	1.2	2.4	1.0	3.5	1.1	1.0	1.3	2.0	4.2	3.9	2.2	1.0	1.2	1.0	1.0

Analyses are from J. Cotten, GDR-GEDO, Université de Bretagne Occidentale, Brest, France.

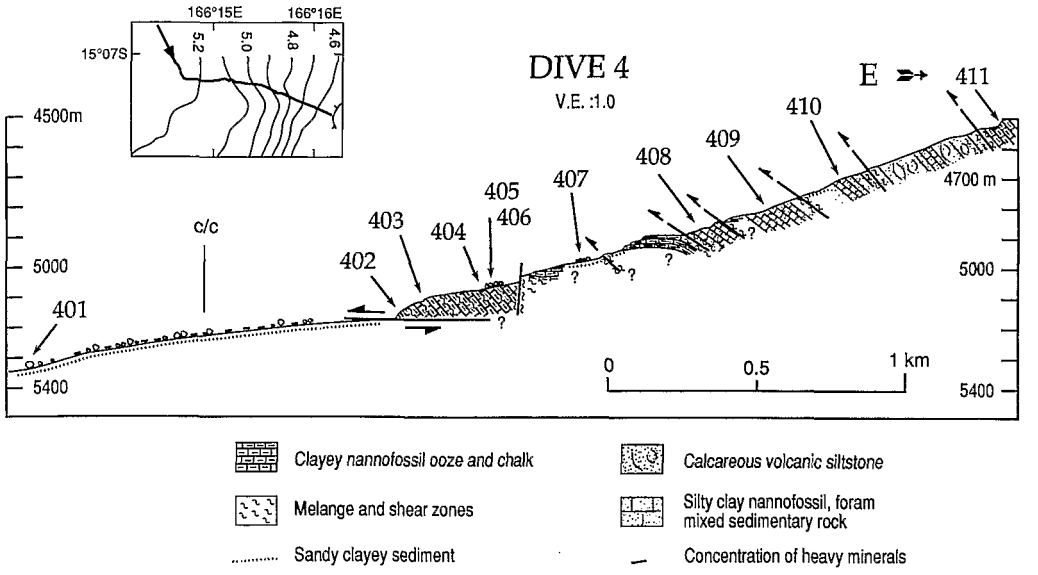

Fig. 5. Interpreted geologic cross-section of the toe of the New Hebrides arc slope north of the North d'Entrecasteaux Ridge (dive 4); location in Fig. 2; inset is *Nautile* traverse; arrows with numbers indicate location of samples described in Table 1.

Close to the contact zone between the arc and the guyot, the platform of the guyot gently dips 8° arcward and shows a 150-m-high bump (dive 6; Fig. 6). In contrast, the upper SE flank of the guyot (dive 5; Fig. 7) dips uniformly 27° eastward.

Limestone outcrops discontinuously between

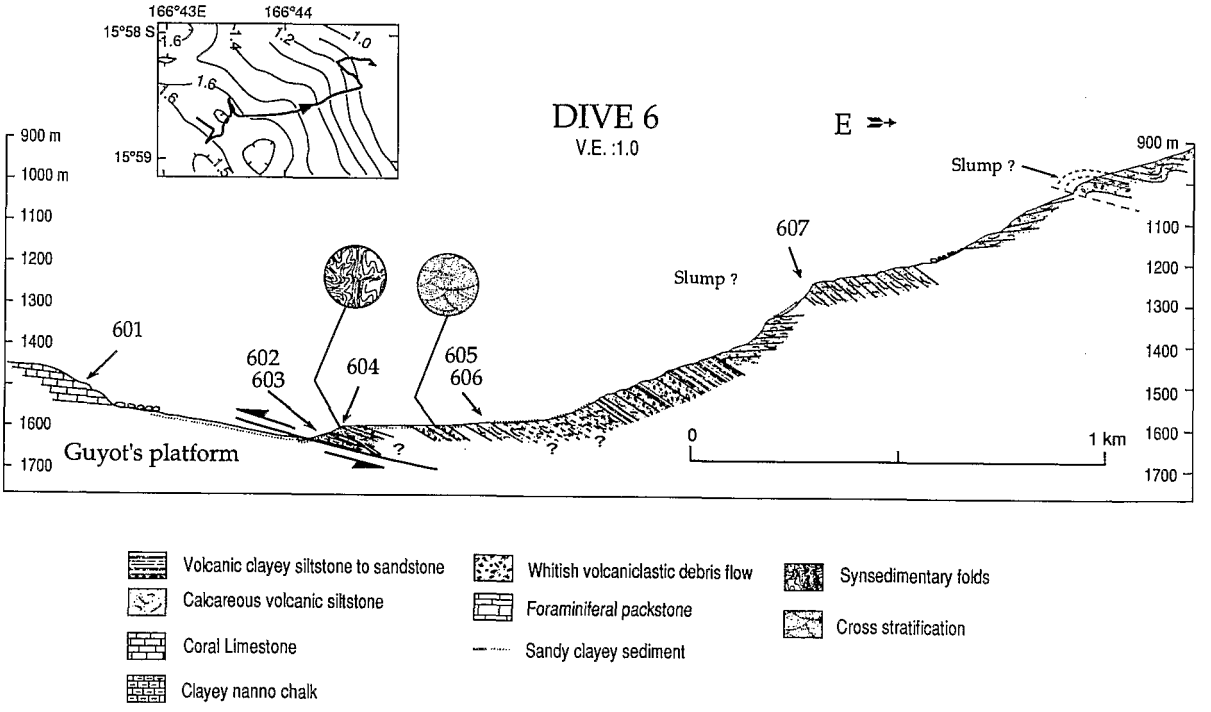

Fig. 6. Interpreted geologic cross-section of the toe of the New Hebrides arc slope that towers above the platform of the Bougainville guyot (dive 6); location in Fig. 2; inset is *Nautile* traverse; arrows with numbers indicate location of samples described in Table 1.

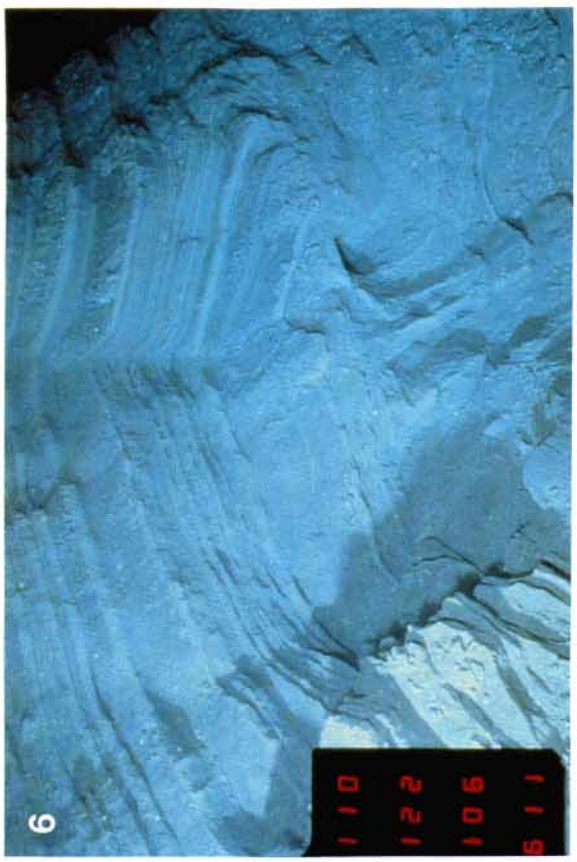
6


8


5


7

1450 m on the platform of the guyot (dive 6) and 2350 m along its SE flank (dive 5). Massive subhorizontal limestone beds are exposed to a height over of 100 m along the eastern slope of the bump (Fig. 6). At the upper SE flank of the guyot (Fig. 7), rare limestone beds, which are 10 cm to 1 m thick, dip consistently 20–30° parallel to the slope.

Reef limestones (Plate I-4) and fragments of coral colony, studied by Montaggioni et al. (1991), attest to a previous reef environment on the guyot during the Late Oligocene to Early Miocene and Latest Miocene to Early Pliocene (Tables 1 and 2). Moreover, strong evidence for diagenetic alteration of corals and reef limestones indicates that the guyot was emergent in the past (Montaggioni et al., 1991).

The oldest rock recovered from the Bougainville guyot was dredged along the guyot's southern flank (D1I, Table 2). This rock, dated from the uppermost Middle Eocene (40–42 Ma), is a coarse volcanic breccia with basaltic clasts and a white chalky matrix. The basaltic clasts appear to be mineralogically identical to the samples of porphyritic island-arc tholeiite D1B and D1C (Tables 2 and 3). Other clasts found in the conglomerate D1J and the breccia D1L (Table 2) indicate deposition of nannofossil ooze on the guyot's flank during the Middle Oligocene.

All igneous samples dredged at site D1 (Fig. 2, Table 2) can be grouped into moderately porphyritic olivine basalt, microcrystalline basalt and highly porphyritic basic andesite. Geochemical analysis suggest that these igneous samples have an island-arc origin and include three main components: Island-Arc Tholeiite (IAT), basic andesite (BA), and andesite (A) (Table 3). Hence, petrologic data clearly indicate that the Bougainville guyot is an island-arc volcano (Fig. 8). Only one sample (D1H, Table 2) was tentatively dated, and yielded a 15 Ma K/Ar minimum age. This age appears very young when compared to the Middle Eocene age of the volcanic breccia recovered from the guyot, although the 15 Ma age might indicate late guyot magmatism.

The arc slope in front of the Bougainville guyot

We first present the geology of the arc slope 15 km north of the indentation (dive 7). Then we summarize the geologic features of the contact zone and focus on two closely spaced cross-sections (dives 5 and 6) that illustrate the lateral variation in the geology and tectonics of the Bougainville guyot–New Hebrides island arc collision zone.

The arc slope north of the guyot's indentation

At the site of dive 7 (Fig. 2), the arc slope is smooth and dips 25°W. This slope is cut by shallow (10 cm–3 m) gullies that trend N50–60° and by 10-m-high scarps that trend N140°. The flanks of the gullies reveal well stratified, 1–20-cm-thick layers of volcaniclastic rocks that dip 20–30° trenchward (Plate II-5, Fig. 9). These rocks, which were deposited during Late Pleistocene and Holocene times, show evidences of clasts of lavas and nannofossil chalk, and reworked Oligocene and Miocene–Pliocene foraminifers. An andesite clast recovered from a volcanic conglomerate (705, Table 3) yielded an Early–Middle Miocene radiometric age (Table 1), the same age as volcanic rocks on Espiritu Santo and Malakula Islands (Mallick and Greenbaum, 1977). Nevertheless, a clast of Oligocene nannofossil chalk (706, Table 1) recovered from a calcareous silty clay is un-

Plate II

5 Late Pleistocene volcanic siltstone and sandstone beds dipping 20–30° trenchward along the New Hebrides Island Arc slope (dive 7, 2018 m).

6 A synsedimentary fold at the toe of the arc slope east of the Bougainville guyot; sediments are stratified calcareous volcanic siltstone and sandstone (dive 6, 1611 m).

7 Fractured fine limestones in a wedge of accreted rocks near the toe of the arc slope in the collision zone between the Bougainville guyot and the New Hebrides island arc (dive 5, 2175 m).

8 Steeply dipping layers of white limestone intercalated with brown sheared sediments that may indicate a zone of tectonic contact in the wedge of accreted rocks east of the Bougainville guyot (dive 5, 2076 m).

known on the nearby islands and might have an exotic origin.

The contact zone between arc and guyot

The contact zone between the guyot's platform and the arc slope (dive 6, Fig. 6) lies along a 300-m-wide depression that is draped with sandy–clayey sediment; no scree was observed in this depression. The seaward flank of this depression exhibits NE-facing, vertical scarplets that are 20–40 cm in height. Along the SE flank of the guyot (dive 5, Fig. 7), the contact zone forms a 10-m-wide, flat-bottomed canyon floored by fine-grained sediment. A N–S-trending, 20-cm-high, scarplet cuts across Recent sediment at the deepest point of the canyon. Scree partially covers both flanks of the canyon (dive 5). Limestone blocks on the western flank of the canyon are topped with dark gray clay, whereas boulders deposited along the eastern flank of the canyon are clay-free. This difference in clay cover suggests active tectonics along the arc side of the canyon. The scarplets that were observed at three locations (dives 2, 5 and 6) along the contact zone probably indicate recent tectonic activity.

The toe of the arc slope east of the Bougainville guyot

The western flank of the arc slope antiform that towers above the guyot's platform dips 35° trenchward and has a rough morphology (dive 6, Fig. 6). The sea floor shows 5–50-m-high scarps dipping 40–80° westward, fresh slump scars and NE-trending deep canyons.

The western flank of the antiform exhibits spectacular outcrops that consist of Late Pliocene to Quaternary interbedded volcanic siltstone (Plate II-6) and sandstone (dive 6, Table 1) with whitish volcaniclastic debris flows (Fig. 6). Volcanic siltstones sampled along this part of the sea floor contain reworked early Middle Miocene and uppermost Miocene nannofossils, similar to those recovered along the arc slope near the NDR.

A few samples of sedimentary rock collected at the base of the flank differ in lithology from the rest of the flank. Among these samples are a

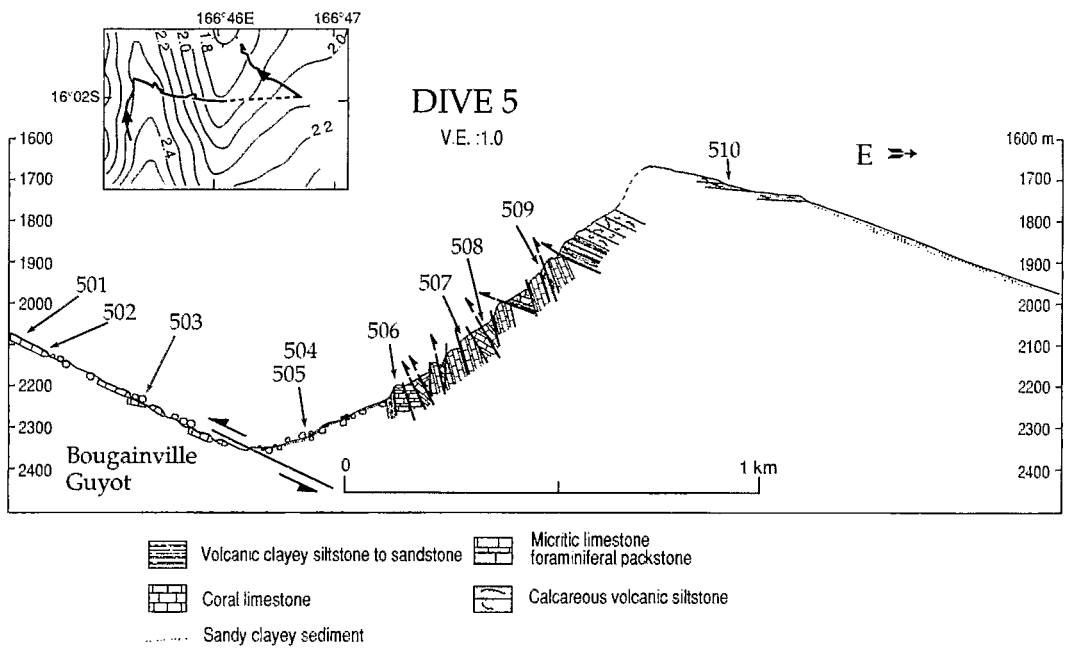

Fig. 7. Interpreted geologic cross-section of the toe of the New Hebrides arc slope southeastward of the Bougainville guyot' s flank (dive 5); location in Fig. 2; inset is *Nautile* traverse; arrows with numbers indicate location of samples described in Table 1.

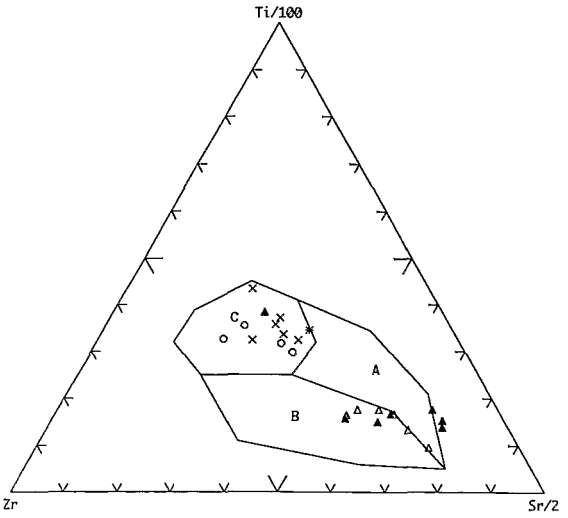

Fig. 8. Compositions of volcanic rocks from the d' Entrecasteaux Zone region reported in a geotectonic triangular plot (Pearce and Cann, 1973). Delineated fields are: *A* = island-arc tholeiite; *B* = calc-alkali basalt; *C* = ocean-floor basalt (MORB). Symbols are: closed triangle = samples from the New Hebrides arc slope (SUBPSO1); the closed triangle in field C is sample 603A (Table 3); open triangle = samples from the Bougainville guyot (SEAPSO1); open circle = samples from the NDR east of 164°E (GEORSTOM 3; Maillet et al., 1983); cross = samples from the NDR west of 164°E (GEORSTOM 3); asterisk = DSDP 286 basement (analyses from Stoeser, 1975).

Miocene–Pliocene pelagic limestone, with sponge spicules (602A, Table 1) that suggests a deep-water, fore-reef environment, and Late Oligocene to Early Miocene nannofossil chalk and limestone (603B and 604B, Table 1). These rocks are very hard, and show shear distortion and an incipient foliation that indicate tectonic deformation.

A pebble of basalt (603A, Table 1) was sampled from the whitish debris flow at the toe of the antiform; this basalt has a MORB affinity (Table 3) that contrasts with island-arc lavas sampled near this area. The source origin of both this sample and the deformed calcareous samples will be discussed further below.

The oldest age determined from rocks anywhere along the arc slope within the study area is late Middle Eocene (46–41 Ma). This age is based on *Globigerinatheka subconglobata euganea*, which is reworked in a Late Oligocene reef packstone (603C, Table 1).

Arc slope rocks that form the western flank of the antiform east of the guyot's platform are tilted wholly arcward and show numerous structures such as folds, slumps and cross-stratifica-

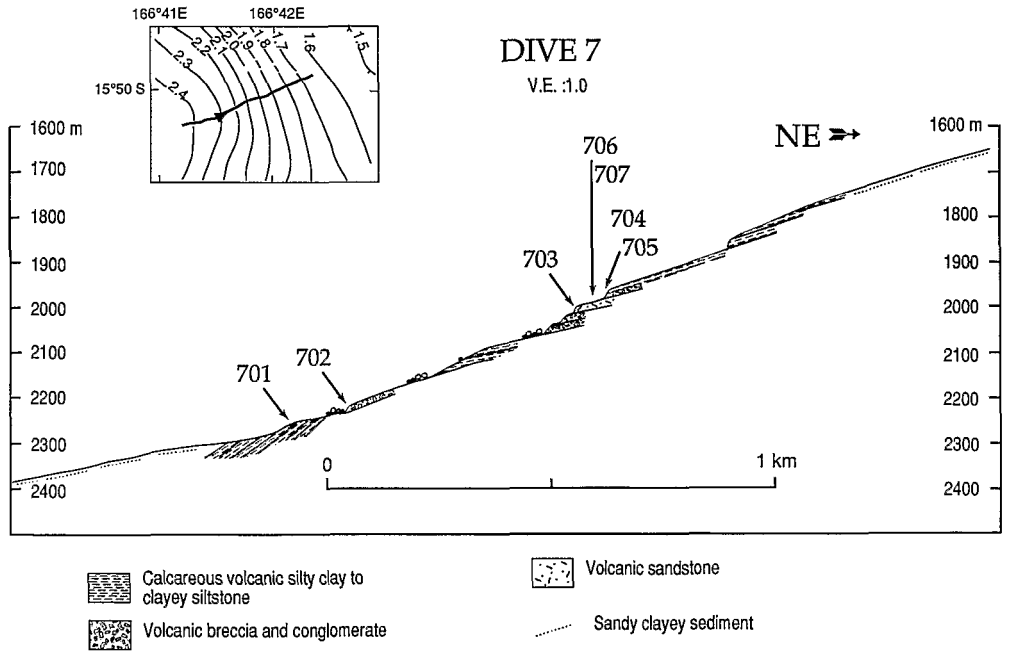

Fig. 9. Interpreted geologic cross-section of a possible slump scar at the New Hebrides arc slope, north of the Bougainville guyot (dive 7); location in Fig. 2; inset is *Nautile* traverse; arrows with numbers indicate location of samples described in Table 1.

tions. Within the lower half of the section (Fig. 6), the rocks dip monoclinally 30–60° arcward, whereas rocks forming the upper half dip alternately arcward and seaward. Either tectonic compression or slumping of rocks could account for the apparently folded layers. Although no clear evidence for shearing was observed within the deformed sedimentary mass, faults between layers of opposite dip cannot be excluded. However, numerous folds ranging in size from 10 cm to several meters affect the arcward dipping layers of the lower half of the section (Plate II-6). The attitude of these folds suggests that they are synsedimentary structures that formed prior to the eastward tilting of the sedimentary mass. We suggest that these folds developed as sediment deposited and slumped on a paleosurface that dipped southwestward.

The arc slope SE of the Bougainville guyot

Southeast of the guyot, where the antiform narrows and deepens (dive 5, Fig. 7), the toe of the arc slope is severely eroded and exhibits the deep structures of the antiform. At this location, the sea floor dips as steeply as 43° west.

The upper third of the cross-section consists of well-stratified, volcanic siltstone that was deposited during Late Pleistocene and Holocene times. Most of the layers dip 40°E, but near the summit of the antiform they dip 30°S.

Calcareous rocks (Plate II-7) outcrop in the lower two-thirds of the section. Locally, these rocks are in tectonic contact with reddish-yellow rocks of uncertain origin. Nevertheless, a sample of volcanic and foraminiferal sandstone (505, Table 1) collected from a scree slope (Fig. 7) may represent these reddish-yellow rocks. This sandstone formed in a reef environment during the Late Eocene to Early Oligocene (Montaggioni et al., 1991). The calcareous rocks include, very hard, micritic limestone (504 and 506, Table 1) and reef packstone (507 and 508, Table 1). Similar to the reef packstone collected on the guyot, sample 508 shows evidences for meteoric diagenesis (Montaggioni et al., 1991). Reef packstone 507, which includes reworked Late Eocene large benthic foraminifers, is of Late Oligocene to Early Miocene age (Montaggioni et al., 1991).

Rocks of the lower two-thirds of the arc slope explored during dive 5 are highly tectonized. The bedding strikes primarily NW–SE and dips variably between 50 and 80°NE. These rocks are fractured and show discrete zones of intense shearing that are interpreted as reverse and thrust faults (Plate II-8, Fig. 7). Samples of micritic limestone and reef packstone bear the mark of folding and stretching. Two groups of subvertical faults and fractures that trend respectively N20° and E–W suggest conjugate faulting. The trends of faulting are consistent with a maximum horizontal compression oriented N50°E ± 10°, whereas the plate convergence direction is N76° ± 11° (Isacks et al., 1982). Horizontal striations on a vertical fault plane (slickensides?) substantiate strike-slip motion along the fault. The tectonic deformation strongly decreases above 1850 m in the upper third of the section.

Discussion

The Bougainville guyot: a Middle Eocene island-arc volcano

The dredged volcanic breccia D11 (Table 2) shows that the Bougainville guyot formed as an island-arc volcano prior or during the latest Middle Eocene. Cores collected at DSDP site 286, 50 km SW of the guyot, revealed an uppermost Middle Eocene andesitic conglomerate that overlays Middle Eocene vitric andesitic siltstone and sandstone that was deposited on the basaltic oceanic crust (Andrews et al., 1975; Stoeser, 1975). Multichannel seismic reflection data that tie the area of Site 286 to the South d'Entrecasteaux Chain (SDC) show that stratas, including the andesitic conglomerate, thicken from this site toward the SDC (Fisher, 1986; pp. 10,479–10,480) suggesting that these rocks were derived from the SDC. Hence, the breccia dredged at the Bougainville guyot, together with the sequence drilled at DSDP Site 286, suggest that the guyot formed during the Middle Eocene.

The petrology and Middle Eocene age of the Bougainville guyot imply that when the North Loyalty basin was an active marginal basin (Weis-

sel et al., 1982; Andrews et al., 1975), island-arc volcanism was active along its northern edge. This volcanism occurred in conjunction with a possible south-dipping subduction zone that extended along the north side of the NDR (Burne et al., 1988). The SDC grew on the DEZ's crust, which is scarcely thicker (12–14 km, Collot and Fisher, 1988) than that of the North Loyalty basin (10–12 km, Pontoise et al., 1982) and is not typical of a well developed island-arc crust (24–25 km, Ibrahim et al., 1980). Therefore, the SDC can be regarded either as an island arc that aborted early or as the poorly developed western end of a mature island arc that is now subducted beneath the New Hebrides arc.

Montaggioni et al. (1991) used the facies and biostratigraphic analysis of the carbonate samples to suggest that during the Middle and Late Miocene the deposition of reef limestones was interrupted by a phase of low sea level or cooling. The deposition of reef limestones on the guyot appears to have ceased some time after the Early Pliocene. This cessation is in agreement with the recent drowning of the guyot, which was transported from the sea level down to the trench as suggested by the models of Dubois et al. (1988).

Geology of the forearc slope offshore Espiritu Santo island

Four major groups of lithologies were identified along the forearc slope west of Espiritu Santo island, and consist of (1) lavas and peridotite, (2) volcaniclastic rocks and sediments, (3) nannofossil ooze and chalk, and (4) lagoon and reef limestones. The first two groups include lithologies that mainly originated from the New Hebrides island arc, whereas the other two may have been accreted from the downgoing plate, as discussed further below.

Massive andesites and andesitic basalts encountered in the upper part of the arc slope (dive 1) probably represent the volcanic New Hebrides arc basement. However, the unique 7.3 Ma K/Ar date obtained from an andesitic basalt has no equivalent on Espiritu Santo island, but this date is similar to the 10.7–7.5 Ma ages that were determined from volcanic rocks in SE Malakula island (Macfarlane et al., 1988). Andesite and island-arc tholeiite clasts sampled from conglomerates and breccias along the arc slope (samples 318 and 705, Table 3) could also have been derived from the New Hebrides island arc. These samples yielded an Early-Middle Miocene radiometric age (Table 2), which is consistent with the Early and lower Middle Miocene island-arc volcanism which is known to have occurred on Espiritu Santo and Malakula islands (Mallick and Greenbaum, 1977).

A microlitic basalt with MORB affinity collected at the toe of the arc slope near the platform of the guyot (603A, Table 3, Fig. 8) may substantiate the hypothesis of accretion from the downgoing plate. Indeed no a such type of basalt is known on the New Hebrides Island Arc, but the basement of the DEZ is MORB (Fig. 8). Although it is likely that this basalt was accreted from the oceanic crust of the DEZ, the 9.4 Ma K/Ar age of the sample, which is a minimum age, does not appear realistic with respect to the 36–56 Ma age of the DEZ basement (Maillet et al. 1983).

A lherzolite fragment (606, Table 3) recovered at the base of the arc slope east of the Bougainville guyot (dive 6) is of uncertain geographic origin. The only peridotites known on the New Hebrides islands are exposed along the eastern belt, on Pentecost island (Mallick and Neef, 1974). This fragment could have been transported from the eastern belt area along a sediment pathway that was later closed off by the uplift of the western belt. Alternatively, the location of the lherzolite sample on the forearc slope could indicate that the two converging lithospheres have been deeply affected by the tectonic effects of the collision; in this respect, the sample could have been evenly thrust up from the deep crust of the downgoing plate or from that of the western belt.

Pliocene–Quaternary volcaniclastic rocks and sediments appear to be locally important in volumetric terms, because they were observed over hundreds of meters of thickness at all of the dive sites. The composition of these rocks and sediments suggests that they derive from the nearby island arc. For example, volcanic sandstone en-

cases island-arc volcanic clasts and results locally from an almost pure accumulation of island-arc volcanic debris (301 and 703, Tables 1 and 3).

The Pliocene–Quaternary volcaniclastic rocks and sediments include early Middle Miocene nannofossils (samples 304A, 311 and 602B, Table 1) and latest Miocene clasts of chalk (sample 306) that could either be reworked from the island arc or from sediments that were accreted from the downgoing plate. However, these Miocene nannofossils and clasts of chalk are difficult to relate to sediments from the downgoing plate, because at DSDP site 286 most of the Miocene is absent and only questionable Early Miocene abyssal red clay is present (Andrews et al., 1975). In contrast, the reworked early Middle Miocene nannofossils are coeval with a thick greywacke formation that outcrops on Espiritu Santo island (Macfarlane et al., 1988) and the latest Miocene clasts of chalk resemble the Late Miocene to earliest Pliocene calcarenite exposed on this same island (Fig. 2; Mallick and Greenbaum, 1977; Carney et al., 1985). Therefore the miocene microfossils and clasts reworked in Pliocene–Quaternary volcaniclastic rocks and sediments could be derived from the island arc.

The total absence of reworked late Middle to early Late Miocene nannofossils in rock samples that contain early Middle (NN4–5) and latest Miocene (NN11) nannofossils (Table 1) is considered significant of a hiatus that extended between 14 and 8 Ma. In this hypothesis the hiatus roughly correlates in time to the 11–8 Ma uplift and erosion phase that affected the western belt (Carney et al., 1985, Macfarlane et al., 1988) and to the Middle–Late Miocene hiatus recorded at DSDP Site 286 (Andrews et al., 1975).

Clayey nannofossil ooze, chalk and limestone of Middle Oligocene to Early Miocene were encountered at the toe of the arc slope, north of the NDR (dive 4) and to a lesser extent east of the Bougainville guyot (dive 6). These sediments locally contain Eocene nannofossils and differ from the uppermost Oligocene to Lower Miocene, coarse volcaniclastic deposits exposed on Espiritu Santo island (Mallick and Greenbaum, 1977). In contrast, these deep-water sediments are similar in age and facies to the Oligocene nannofossil ooze and uppermost Eocene chalk cored at DSDP Site 286 (Andrews et al., 1975). The deep-water rocks and sediments collected at the arc slope and at Site 286 both contain sponge spicules and a small amount of volcanic silt. Although the Early Miocene(?) abyssal red clays cored at Site 286 were not recovered at the toe of the arc slope, we suggest that the Middle Oligocene to Early Miocene deep-water sediments were accreted from the Australian plate to the arc slope.

Reef and micritic limestones are the major components of a 500-m-thick wedge accreted within the arc slope antiform east of the Bougainville guyot (dive 5). This wedge also includes minor volcanic siltstone and sandstone that was tectonically emplaced between thrust sheets of reef and micritic limestones (Fig. 7). A Late Oligocene to Early Miocene reef limestone (507) collected within this wedge is equivalent in age and lithology to those dredged from the guyot, but the limestone from the wedge could also be correlated with Late Oligocene to Early Miocene lenses of reef limestones exposed on the western belt of islands (Mallick and Greenbaum, 1977; Mitchell, 1966, 1971). However, the reef limestone recovered from the wedge includes reworked Late Eocene large benthic foraminifers, indicative of reef material similar to that discovered about 200 km further east, on Maewo island within an Early Miocene conglomerate (Coleman, 1969). This reef material may have been transported from Maewo island to the forearc prior to the uplift of the western belt. This hypothesis is unlikely, since these reefal debris are not present in the western belt. Such Late Eocene foraminifers were not recovered from the Bougainville guyot either. However, a Middle Eocene age was determined from the guyot (D11, Table 2) and the toe of the arc slope (603C, Table 1), but is unknown on the New Hebrides island arc. Hence, because of equivalent Late Oligocene to Early Miocene reef limestone and similar Middle Eocene age found on both the guyot and the toe of the arc slope, and because the wedge of imbricated reef limestone was only encountered in front of the guyot, we suggest that this wedge accreted from the guyot or a previously subducted one.

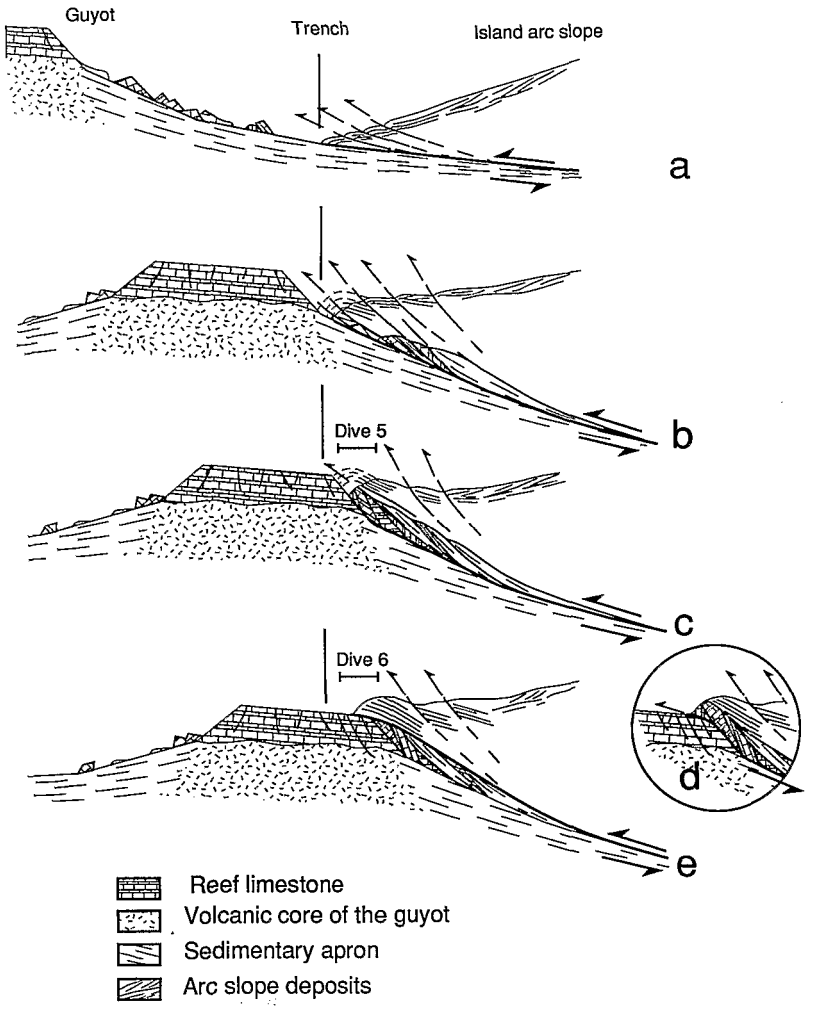

Fig. 10. Schematic diagram showing the early stages of subduction of a guyot. The heavy line is the inter-plate décollement. (a) The arc slope shortens by internal thrusting. (b,c) Limestones of the guyot's cap and sediments of the debris apron that flanks the guyot are thrust up and form an imbricated wedge beneath the arc slope; this wedge tends to smooth the slope breaks of the leading flank of the guyot. (d) Insert showing the imbricated wedge accreted to the arc and overthrusting the guyot's cap; this situation was not observed during the dives. (e) An alternate situation interpreted from dives 5 and 6: the décollement shifted upward from the guyot's flank to the top of the wedge, so that the imbricated wedge does not accrete to the arc slope; this process would deform the guyot into an elongated feature and facilitate its subduction.

The early stage of collision between a seamount or a ridge and arc

The models of arc–seamount collision proposed by Lallemand and Le Pichon (1987), Yamazaki and Okamura (1989) and Von Huene and Lallemand (1990) predict that, in the early stages of the collision, compressive thickening affects the toe of the arc slope. Geologic data collected in the DEZ–arc collision zone support this model and emphasize mechanisms such as shortening and tectonic erosion, by which the arc slope accommodates the early stages of seamount or ridge subduction (Fig. 10). For example, where the lower northern flank of the NDR enters the subduction (Fig. 5), highly sheared and upturned rocks and sediments with fresh fractures suggest active shortening of the arc slope by collision. Fresh slump scars and steep slopes incised by deep canyons support active erosion along the deformation front.

A mechanism that facilitates seamount subduction is offsetting of the seamount by normal

faults induced by flexure of the oceanic plate before subduction (Fryer and Smoot, 1985, Ballance et al., 1989; Pelletier and Dupont, 1990). For example, the Daiichi–Kashima seamount that is subducting in the Japan trench is split into two halves by a 1600-m-high normal fault (Kobayashi et al., 1987; Cadet et al., 1987). Although the Bougainville guyot is analogous to the Daiichi–Kashima seamount in volume and position with respect to the trench, the guyot is not dissected by such a large normal fault. Fisher et al. (1991b), drawing an analogy between features of glacial origin and the subduction of the Bougainville guyot, suggest that the guyot's subduction may be facilitated by an eventual evolution of the high-drag shape of the guyot into a more streamlined shape during the collision process. One feature of the high-drag shape of the guyot that is eventually smoothed during the collision is the steep (40–45°), 700-m-high scarp that bounds the guyot's carbonate cap and towers over the gently sloping (5–10°) lower flank of the guyot. The nature and extent of smoothing and deformation caused by the collision depends on the contrast in compressibility between guyot and arc rocks, as discussed by Fisher et al. (1991b). Geologic data presented in this report support the shape evolution of the guyot during the collision, as discussed hereafter.

Geologic samples and observations collected during dive 5 (Fig. 7) indicate a 500-m-thick wedge of accreted reef limestones that imbricated within the arc slope antiform, east of the guyot. Examination of rock deformation at the location of dive 5 shows that the intense tectonic deformation that affects the imbricating layers strongly decreases near 1850 m water depth, in the well-layered, calcareous, volcanic siltstone and sandstone of the upper third of the observed section. This upward decrease of the intensity of deformation suggests that the major thrust fault, i.e. the inter-plate décollement, is located near the base of the imbricating layers. Hence, the reef limestones that probably derived from the guyot's cap were probably scraped off and thrust up the guyot's leading flank, along the inter-plate décollement, as the guyot enters the subduction zone (Figs. 10a–c). Moreover, multichannel seismic reflection data collected across the arc slope, east of the guyot, image thrust faults that cut through highly reflective rocks with parallel bedding, suggesting that sedimentary layers may have been stripped from the debris apron of the guyot and incorporated into the imbricating layers (Fisher et al., 1991b). Sandstone pinched between the accreted limestones (Fig. 7) may be evidence for sediments stripped off the guyot apron, although the sandstone may be derived from the arc. Despite this uncertainty, material accreted east of the guyot forms imbricating layers that tend to smooth out slope breaks in the leading flank of the guyot (Fig. 10c).

Whether the imbricating layers joined rocks of the island arc or became plastered against the leading flank of the guyot and now move with it remains a critical problem (Fisher et al., 1991b). Conceptually, if the 500-m wedge of imbricating layers that outcrops southeast of the guyot was accreted to the arc slope, the wedge should have been thrust up along the décollement until the wedge overthrust the carbonate cap of the guyot (Fig. 10d). This cap extends for about 1 km eastward beneath the antiform, as indicated by multichannel seismic data (Fisher et al., 1991b); nevertheless, observations made during dive 6 (Fig. 6) do not show evidence for imbricating layers exposed at the western flank of the antiform but, rather, show steep, several hundred meters thick outcrops of layered volcanic sediments derived from the arc. However, the few sheared calcareous rocks that were sampled (602A, 603B and 604B, Table 1) near the contact zone between the arc and the platform of the guyot suggest that minor (10 cm–1 m(?) thick), imbricating layers could be buried beneath sandy-clayey deposits and pinched at the very toe of the arc slope. Therefore, the absence of a thick wedge of imbricating layers overthrusting the guyot's cap can be interpreted to suggest that the imbricating layers plastered against the leading flank of the guyot and, conversely, that the décollement migrated upward from the guyot's flank to the top of the wedge (Fig. 10e). In this interpretation, the plastered wedge of imbricating layers deforms the guyot into an elongated feature and hence should facilitate its subduction. Sandbox experimental

modeling (Malavieille and Calassou, 1992) supports the idea of a wedge plastered between arc and seamount that tends to smooth the décollement.

Conclusions

Observations and geologic samples collected in the collision zone between the New Hebrides island arc and the DEZ provide constraints about the age and lithology of the Bougainville guyot and forearc slope rocks, as well as support for the mechanisms that control the subduction of a ridge or a seamount. The Bougainville guyot consists of an island-arc tholeiite and andesite core formed during the Middle Eocene, which was later capped by reef limestones. The guyot has had a complex and still partially known subsidence story, the major elements of which deduced from dredging are as follows: two periods of reef limestone deposition (Late Oligocene to Early Miocene, and latest Miocene to Early Pliocene), which appear to be separated by a Middle–Late Miocene period of emergence. The forearc slope in the DEZ–New Hebrides island arc collision zone is characterized by various lithologies and structures, and bears the marks of the collision. The upper arc slope consists of fractured Miocene volcanic arc basement and Pliocene–Pleistocene trenchward-dipping, volcaniclastic deposits that appear to derive from onshore. The time of the volcaniclastic deposition coincides with the Pliocene to Recent uplift phase of Espiritu Santo island. In the lower part of the arc slope, arc-derived volcaniclastic sediments adjacent to the NDR were fractured, tilted northward and eroded as a result of the collision. Above the Bougainville guyot's platform, volcaniclastic sediments were strongly tilted arcward; those sediments that were fractured may have been removed, by erosion, producing a 10-km indentation in the arc slope. At the toe of the arc slope, against the northern flank of the NDR, highly sheared, Middle Oligocene to Early Miocene nannofossil ooze and chalk probably accreted from the downgoing plate. Similarly, in front of the Bougainville guyot, a 500-m-thick wedge of imbricating layers of Late Oligocene to Early Miocene reef and micritic limestones probably accreted from the guyot or a previously subducted one. This wedge that accumulates ahead of the guyot beneath the lower arc slope rocks can be interpreted as moving downward with the guyot, and thus facilitating its subduction by streamlining.

Acknowledgements

We gratefully acknowledge the captain and crew of the *R.V. Nadir* and the pilots of the submersible *Nautile* for their invaluable help during the cruise. We also thank J.M. Auzende, C. Blot, S. Uyeda and Y. Ogawa for their scientific comments and help in improving the manuscript.

References

Andrews, J.E. et al., 1975. Site 286. Init. Rep. DSDP, 30: 69–131.

Auzende, J.-M., Lafoy, Y. and Marsset, B., 1988. Recent geodynamic evolution of the North Fiji Basin (southwest Pacific). Geology, 16: 925–929.

Ballance, P.F., Scholl, D.W., Vallier, T.L., Stevenson, A.J., Ryan, H., Quiterno, P., Blome, C., Barron, J.A., Bukry, D., Cawood, P.A., Chaproniere, G.C.H., Herzer, R.H. and Tappin, D.R., 1989. Subduction of a late Cretaceous seamount of the Louisville ridge at the Tonga trench—accretion, arc fragmentation, and accelerated subduction erosion. Tectonics, 8: 953–962.

Berggren, W.A., Kent, D.V., Flynn, J.J. and Van Couvering, J.A., 1985. Cenozoic geochronology. Geol. Soc. Am. Bull., 96: 1407–1418.

Burne, R., Collot, J.-Y. and Daniel, J., 1988, Superficial structures and stress regimes of the downgoing plate associated with subduction–collision in the central New Hebrides arc (Vanuatu). In: H.G. Greene and F.L. Wong (Editors), Geology and Offshore Resources of Pacific Island Arcs—Vanuatu Region. Circum-Pacific Council for Energy and Minerals Resources, Houston, Texas, pp. 357–376.

Cadet, J. -P., Kobayashi, K., Aubouin, J., Boulegue, J., Deplus, C., Dubois, J., von Huene, R., Jolivet, L., Kanazawa, T., Kasahara, J., Koizumi, K., Lallemand, S., Nakamura, Y., Pautot, G., Suyehiro, K., Tani, S., Tokuyama, H. and Yamazaki, T., 1987. The Japan trench and its juncture with the Kurile trench: Cruise results of the Kaiko project, Leg 3. Earth Planet. Sci. Lett., 83: 267–284.

Carney, J.N. and Macfarlane, A., 1978. Lower to middle Miocene sediments on Maewo, New Hebrides, and their relevance to the development of the outer Melanesian arc system. Bull. Austral. Soc. Explor. Geophys., 9: 123–130.

Carney, J.N. and Macfarlane, A., 1980. A sedimentary basin in the central New Hebrides arc. UN ESCAP, CCOP/SOPAC, Tech. Bull., 3: 109–120.

Carney, J.N. and Macfarlane, A., 1982. Geological evidence bearing on the Miocene to Recent structural evolution of the New Hebrides arc.Tectonophysics, 87: 147–175.

Carney, J.N., Macfarlane, A. and Mallick, D.I.J., 1985. The Vanuatu Island arc: an outline of the stratigraphy, structure, and petrology. In: A.E.M. Nairn, Frances G. Stehli and S. Uyeda (Editors), The Ocean Basins and Margins, 7A. Plenum Press, New York, N.Y., pp. 683–718.

Chase, C.G., 1971. Tectonic history of the Fiji plateau. Geol. Soc. Am. Bull., 82: 3087–3109.

Coleman, P.J., 1969. Derived Eocene larger foraminifera on Maewo, eastern New Hebrides, and their southwest Pacific implications. In: New Hebrides Anglo-French Condominuim. Annual Report of the Geological Survey for the year 1967, pp. 36–37.

Collot, J.-Y. and Fisher, M.A., 1988. Crustal structure, from gravity data, of a collision zone in the central New Hebrides island arc. In: H.G. Greene and F.L. Wong (Editors), Geology and Offshore Resources of Pacific Island Arcs—Vanuatu Region. Circum-Pacific Council for Energy and Minerals Resources, Houston, Texas, pp. 125–140.

Collot, J.-Y. and Fisher, M.A., 1989. Formation of forearc basins by collision between seamounts and accretionary wedges: an example from the New Hebrides subduction zone. Geology, 17: 930–933.

Collot, J.-Y. and Fisher, M.A., 1991. The collision zone between the north d'Entrecasteaux ridge and the New Hebrides island arc: part 1: Seabeam morphology and shallow structure. J. Geophys. Res., 96: 4457–4478.

Collot, J.Y., Daniel, J. and Burne, R.V., 1985. Recent tectonics associated with the subduction/collision of the d'Entrecasteaux zone in the central New Hebrides. Tectonophysics, 112: 325–356.

Collot, J.-Y., Pelletier, B., Boulin, J., Daniel, J., Eissen, J.-P., Fisher, M.A., Greene, H.G., Lallemand, S. and Monzier, M., 1989. Premiers résultats des plongées de la campagne SUBPSO1 dans la zone de collision des rides d'Entrecasteaux et de l'arc des Nouvelles-Hébrides. C. R. Acad. Sci., Paris, 309: 1947–1954.

Daniel, J. and Katz, H.R., 1981. d'Entrecasteaux zone, trench and western chain of the central New Hebrides island arc: their significance and tectonic relationship. Geo. Mar. Letts., 1: 213–219.

Daniel, J., Collot, J.-Y., Monzier, M., Pelletier, B., Butscher, J., Deplus, C., Dubois, J., Gérard, M., Maillet, P., Monjaret, M.-C., Récy J., Renard, V., Rigolot P. and Temakon, S.J., 1986. Subduction et collisions le long de l'arc des Nouvelles-Hébrides (Vanuatu): résultats préliminaires de la campagne SEAPSO (Leg 1). C. R. Acad. Sci., Paris, 303: 805–810.

Dubois, J., Deplus, C., Diament, M., Daniel, J. and Collot, J.-Y., 1988. Subduction of the Bougainville seamount (Vanuatu): mechanical and geodynamic implications. Tectonophysics, 149: 111–119.

Falvey, D.A., 1975. Arc reversals, and a tectonic model for the North Fiji Basin. Bull. Austral. Soc. Explor. Geophys., 6: 47–49.

Fisher, M.A., 1986. Tectonic processes at the collision of the d'Entrecasteaux zone and the New Hebrides island arc. J. Geophys. Res., 91: 10, 470–10, 486.

Fisher, M.A., Collot, J.-Y. and Geist, E.L., 1991a. The collision zone between the north d'Entrecasteaux ridge and the New Hebrides island arc: part 2, structure from multichannel seismic data. J. Geophys. Res., 96: 4479–4495.

Fisher, M.A., Collot, J.-Y. and Geist, E., 1991b. Structure of the collision zone between the Bougainville guyot and the accretionary wedge of the New Hebrides island arc, Southwest Pacific. Tectonics, 10: 887–903.

Fisher, M.A., Collot, J.-Y. and Smith, G.L., 1986. Possible causes for structural variation where the New Hebrides island arc and the d'Entrecasteaux zone collide. Geology, 14: 951–954.

Fryer, P. and Smoot, N.C., 1985. Processes of seamount subduction in the Mariana and Izu-Bonin trenches. Mar. Geol., 64: 77–90.

Greene, H.G., Macfarlane, A. and Wong, F.L., 1988. Geology and offshore resources of Vanuatu—introduction and summary. In: H.G. Greene and F.L. Wong (Editors), Geology and Offshore Resources of Pacific Island Arcs—Vanuatu Region. Circum-Pacific Council for Energy and Minerals Resources, Houston, Texas, pp. 1–25.

Greene, H.G., Collot J. -Y., Pelletier B. and Lallemand S., 1992. Observations of forearc seafloor deformation along the North d'Entrecasteaux Ridge—New Hebrides Island arc Collision Zone from Nautile submersible. Init. Rep. Ocean Drilling Program, Leg 134. College Station, Texas, pp. 259–546.

Ibrahim, A.K., Pontoise, B., Latham, G., Larue, M., Chen, T., Isacks, B., Récy, J. and Louat, R., 1980. Structure of the New Hebrides arc-trench system. J. Geophys. Res., 85: 253–266.

Isacks, B.L., Cardwell, R.K., Chatelain, J.-L, Barazangi, M., Marthelot, J.-M., Chinn, D. and Louat, R., 1981. Seismicity and tectonics of the central New Hebrides island arc. In: D.W. Simpson and P.G. Richards (Editors), Earthquake Prediction and International review. American Geophysical Union, Washington, D.C., pp. 93–116.

Jouannic, C., Taylor, F.W., Bloom, A.L. and Bernat, M., 1980. Late Quaternary uplift history from emerged reef terraces on Santo and Malekula Islands. UN ESCAP, CCOP/SOPAC Tech. Bull., 3: 91–108.

Kobayashi, K., Cadet, J.-P., Aubouin, J., Boulègue, J., Dubois, J., von Huene, R., Jolivet, L., Kanazawa, T., Kasahara, J., Koisumi, K., Lallemand, S., Nakamura, Y.P., Suyehiro, K., Tani, S., Tokuyama, H. and Yamazaki, T., 1987. Normal faulting of the Daiichi-Kashima seamount in the Japan trench revealed by the Kaiko I cruise, Leg 3. Earth Planet. Sci. Lett., 83: 257–266.

Kroenke, L.W., Jouannic, C., and Woodward, P., 1983. Bathymetry of the Southwest Pacific. Geophysical Atlas of the Southwest Pacific, 1, pp. 2 sheets.

Lallemand, S. and Le Pichon, X., 1987. Coulomb wedge model applied to the subduction of seamounts in the Japan trench. Geology, 15: 1065–1069.

Louat, R. and Pelletier, B., 1989. Seismotectonics and present-day relative plate motions in the New Hebrides—North Fiji basin region. Tectonophysics, 167: 41–55.

Macfarlane, A., Carney, J.N., Crawford, A.J. and Greene, H.G., 1988. Vanuatu—a review of the onshore geology. In: H.G. Greene and F.L. Wong (Editors), Geology and Offshore Resources of Pacific Island Arcs—Vanuatu Region. Circum-Pacific Council for Energy and Minerals Resources, Houston, Texas, pp. 45–91.

Maillet, P., Monzier, M., Selo, M. and Storzer, D., 1983. The d'Entrecasteaux zone (Southwest Pacific): a petrological and geochronological reappraisal. Mar. Geol., 53: 179–197.

Malahoff, A., Reden, R.H. and Fleming, H.S., 1982. Magnetic anomaly and tectonic fabric of marginal basins north of New Zealand. J. Geophys. Res., 87: 4109- 4125.

Malavieille, J., Calassou, S., Larroque, C., Lallemand, S. and Stéphan, J.-F., 1991. Experimental modelling of accretionary wedges. EUG VI, Strasbourg, March 24–28. Terra Abstracts, 3: p. 367.

Mallick, D.I.J. and Greenbaum, D., 1977. Geology of southern Santo. New Hebrides Geological Survey Report, New Hebrides, pp. 1–84.

Mallick, D.I.J. and Neef, G., 1974. Geology of Pentecost. New Hebrides Geological Survey Report, New Hebrides, pp. 1–103.

Mazzullo, J.M., Meyer A. and Kidd R., 1987. New sediment classification scheme for the Ocean Drilling Program: handbook for shipboard sedimentologist. In: J.M. Mazzullo and A.G. Graham, ODP Tech Note, College Station, Texas, pp. 45–67.

Minster, J.B. and Jordan, T.H., 1978. Present-day plate motions: J. Geophys. Res., 83: 5331–5354.

Mitchell, A.H.G., 1966. Geology of South Malekula. New Hebrides Geological Survey, New Hebrides, pp. 1–42.

Mitchell, A.H.G., 1971. Geology of Northern Malekula. New Hebrides Geological Survey, New Hebrides, pp. 1–56.

Mitchell, A.H.G. and Warden, A.J., 1971. Geologic evolution of the New Hebrides island arc. J. Geol. Soc. Lond., 127: 501–529.

Montaggioni, L., Butterlin J., Glaçon G., Collot J.-Y., Monzier M., Pelletier B., Boulin J., Lallemand S., Daniel J., Faure G., Lauriat-Rage A., Vénec-Peyré M.T., Blondeau A., Lozouet P., Vacelet J. and Babinot J.-F., 1991. Résultats des plongées SUBPSO1 du Nautile: Signification géodynamique des calcaires de plate-forme le long de la zone de subduction des Nouvelles-Hébrides (Sud-Ouest Pacifique). C. R. Acad. Sci., Paris, 313: 661–668.

Pascal, G., Isacks, B.L., Barazangi, M. and Dubois, J., 1978. Precise relocations of earthquakes and seismotectonics of the New Hebrides island arc. J. Geophys. Res., 83: 4957–4973.

Pearce, J.A. and Cann, J.R., 1973. Tectonic setting of basic volcanic rocks determined using trace element analysis. Earth Planet. Sci. Lett., 19: 290–300.

Pelletier, B. and Dupont J., 1990. Effets de la subduction de la ride de Louisville sur l'arc des Tonga–Kermadec. Oceanol. Acta, 10: 57–76.

Pontoise, B., Latham, G.I. and Ibrahim, A.K., 1982. Sismique réfraction: structure de la croûte aux Nouvelles-Hébrides. Trav. Doc. l'ORSTOM, France, 147: 79–90.

Pontoise, B. and Tiffin, D., 1986. Seismic refraction results over the d'Entrecasteaux zone west of the New Hebrides arc. Géodynamique, 2: 109–120.

Stoeser, D.B., 1975. Igneous rocks from leg 30 of the deep sea drilling project. Init. Rep. DSDP, 30, College station, Texas, pp. 401–414.

Taylor, F.W., Jouannic, C. and Bloom, A.L., 1985. Quaternary uplift of the Torres Islands, northern New Hebrides frontal arc: Comparison with Santo and Malekula Islands, central New Hebrides frontal arc. J. Geol., 93: 419–438.

Taylor, F.W., Frohlich, C., Lecolle, J. and Strecker, M., 1987. Analysis of partially emerged corals and reef terraces in the central Vanuatu arc: comparison of contemporary coseismic and nonseismic with Quaternary vertical movements. J. Geophys. Res., 92: 4905–4933.

Taylor, F.W., Isacks, B.L., Jouannic, C., Bloom, A.L. and Dubois, J., 1980. Coseismic and Quaternary vertical tectonic movements, Santo and Malekula Islands, New Hebrides island arc. J. Geophys. Res., 85: 5367–5381.

von Huene, R. and Lallemand, S., 1990. Tectonic erosion along the Japan and Peru convergent margins. Geol. Soc. Am. Bull., 102: 704–720.

Weissel, J.K., Watts, A.B. and Lapouille, A., 1982. Evidence for Late Paleocene to Late Eocene seafloor in the southern New Hebrides basin. Tectonophysics, 87: 243–251.

Yamazaki, T. and Okamura, Y., 1989. Subducting seamounts and deformation of overriding forearc wedges around Japan. Tectonophysics, 160: 207–229.